Gravitational lensing:
A Swiss knife to dissect galaxies !

Dominique Sluse

(Université de Liège, Belgium)

Observatoire de Strasbourg, April 17th 2015

Gravitational lensing:
A Swiss knife to dissect galaxies !

In collaboration with:
F. Courbin, G. Meylan, A. Eigenbrod (EPFL, Lausanne)
T. Anguita , J. Wambsganss, R. Schmidt (U. Heidelberg + U. Andres Bello)
D. Xu, V. Springel (HITS, Heidelberg)
D. Hutsemékers, L. Braibant, J. Surdej, J.-F. Claeskens (Uni. Liège)
P. Schneider, M. Tewes, O. Wucknitz (AIfA, Uni. Bonn, MPIfR)
…

Observatoire de Strasbourg, April 17th 2015

Gravitational lensing: overview

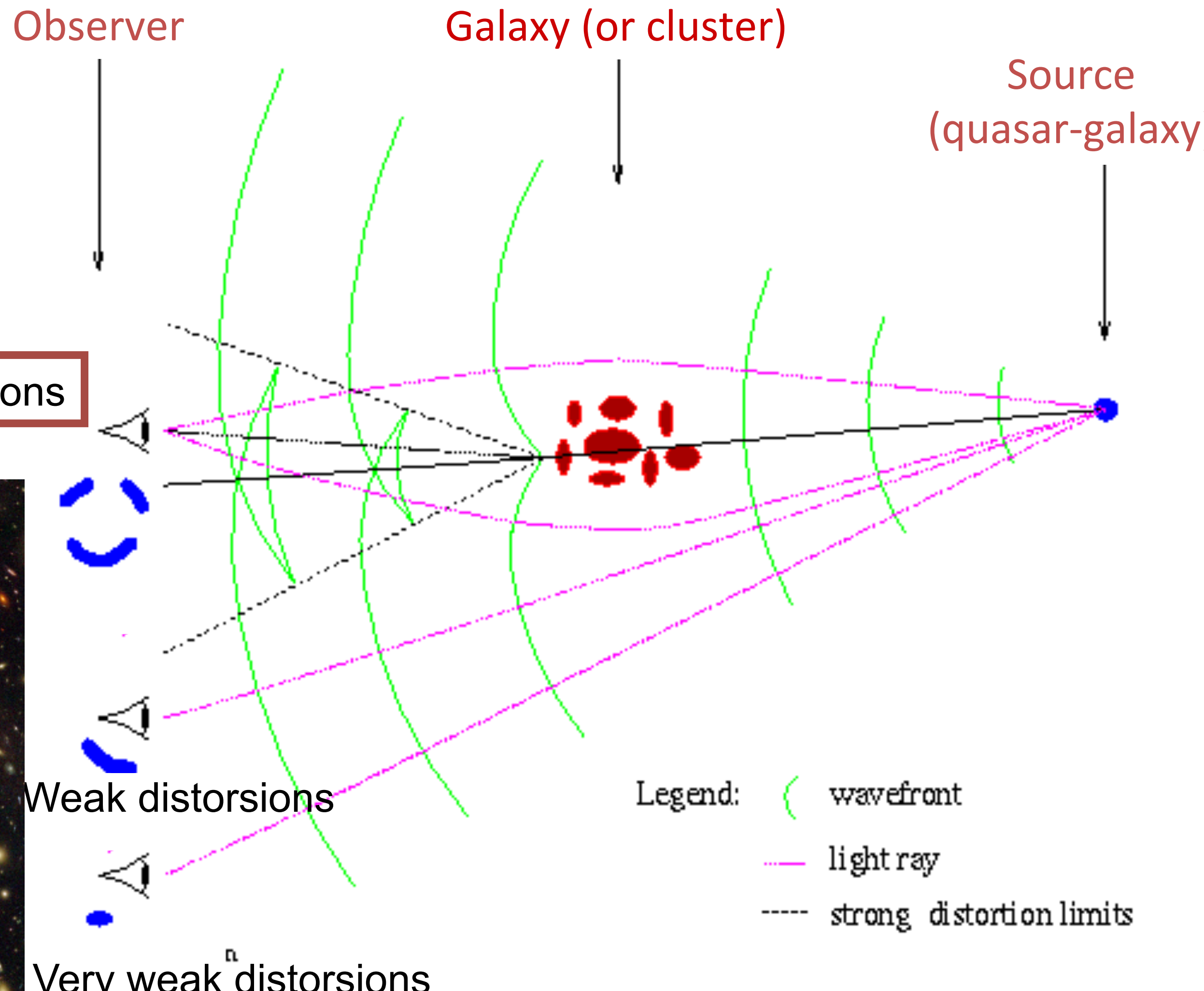

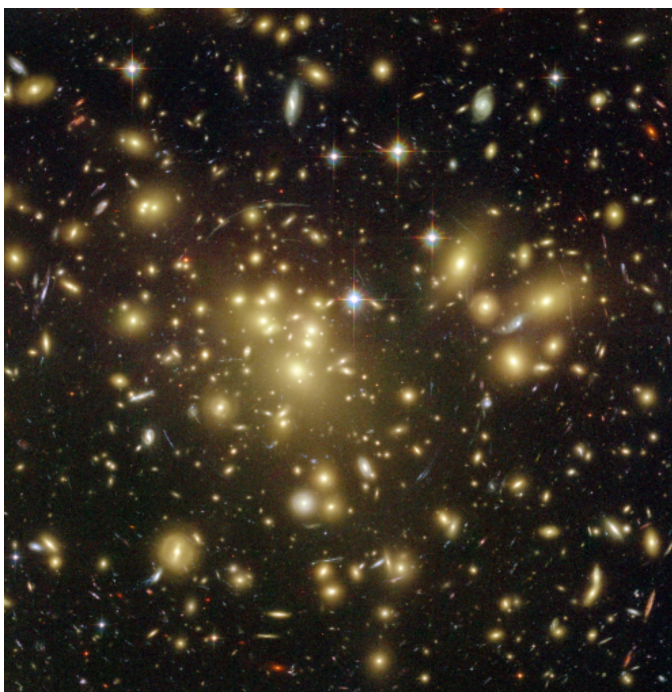

Credit: Fort, Mellier 1994, A&AR, 239, 292

Weighing galaxies

Einstein radius $$\theta_E = \sqrt{\frac{4GM}{c^2}\frac{D_{LS}}{D_L D_S}}$$ = about half of the image separation $\Delta\theta$

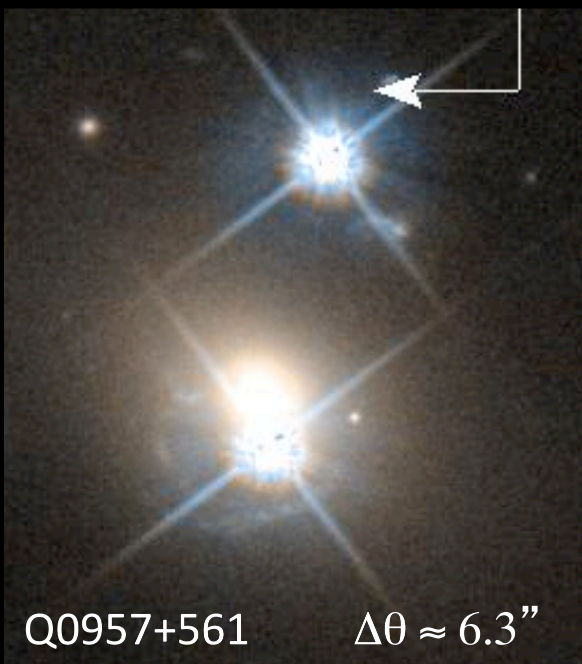

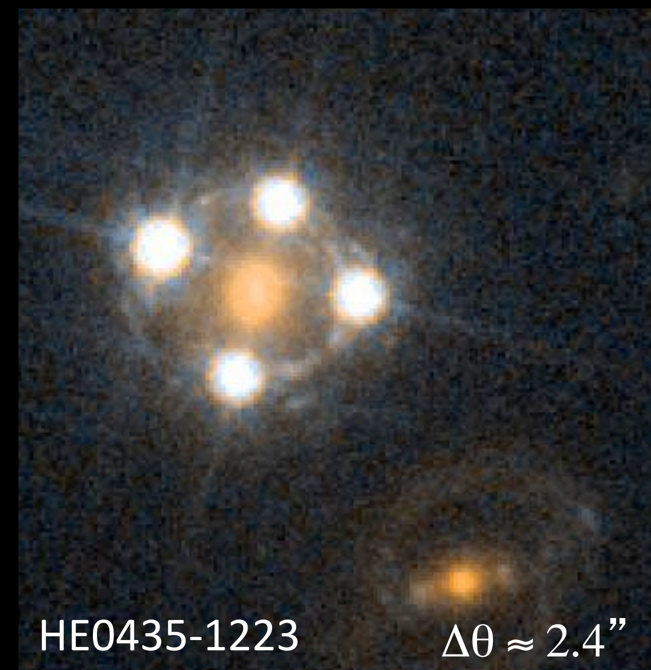

About 130 lensed quasars since 1979, with $R_E = \theta_E/D_{OL} \sim$ 5-10 kpc

Dissecting galaxies with strong gravitational lensing

Measurable quantities

Dependence on the gravitational potential ψ

Time-delay:

$$\tau(\vec{\theta}) = \frac{1}{2}(\vec{\theta} - \vec{\theta_S})^2 - \psi_{2D}(\vec{\theta}).$$

Geometry

ψ

Deflection : (image position)

$$\nabla_{\vec{\theta}}\tau(\vec{\theta}) = 0 \Leftrightarrow (\vec{\theta} - \vec{\theta_S}) = \nabla_{\vec{\theta}}\psi_{2D}(\vec{\theta}) = \vec{\alpha}'(\theta).$$

$\nabla\psi$

Magnification:

$$\mathrm{M}^{-1} \equiv \frac{\partial\vec{\theta_S}}{\partial\vec{\theta}} \equiv \nabla\nabla_{\vec{\theta}}\tau(\vec{\theta}) \equiv \begin{pmatrix} 1 - \frac{\partial^2\psi}{\partial\theta_x} & -\frac{\partial^2\psi}{\partial\theta_x\partial\theta_y} \\ -\frac{\partial^2\psi}{\partial\theta_x\partial\theta_y} & 1 - \frac{\partial^2\psi}{\partial\theta_y} \end{pmatrix}$$

$\nabla\nabla\psi$

Example of lightcurve and time-delay measurement with COSMOGRAIL

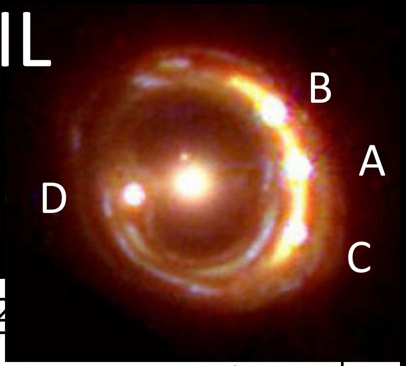

How do we measure time-delays ? With which accuracy ?

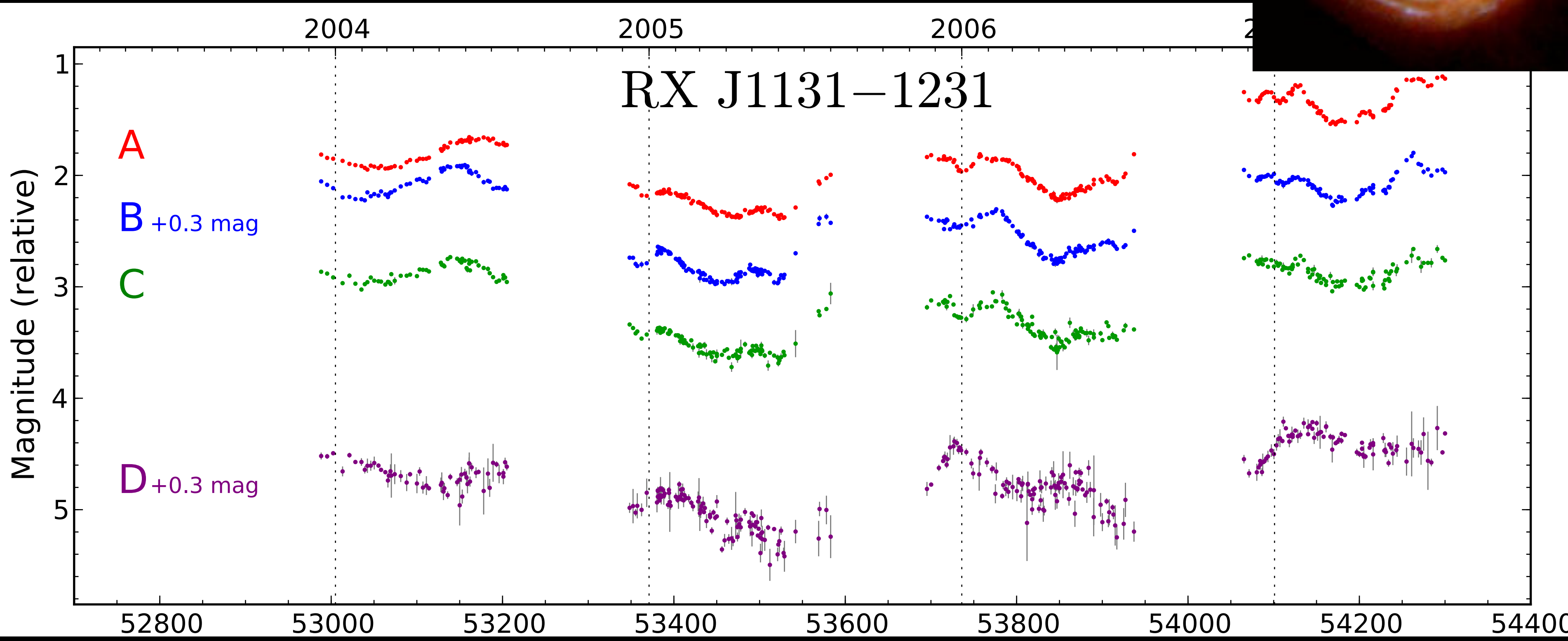

COSMOGRAIL = 30 systems currently monitored with 1m-class telescope

Tewes, …, Sluse 2013, A&A, 556, A22

Example of lightcurve for time-delay measurement with COSMOGRAIL

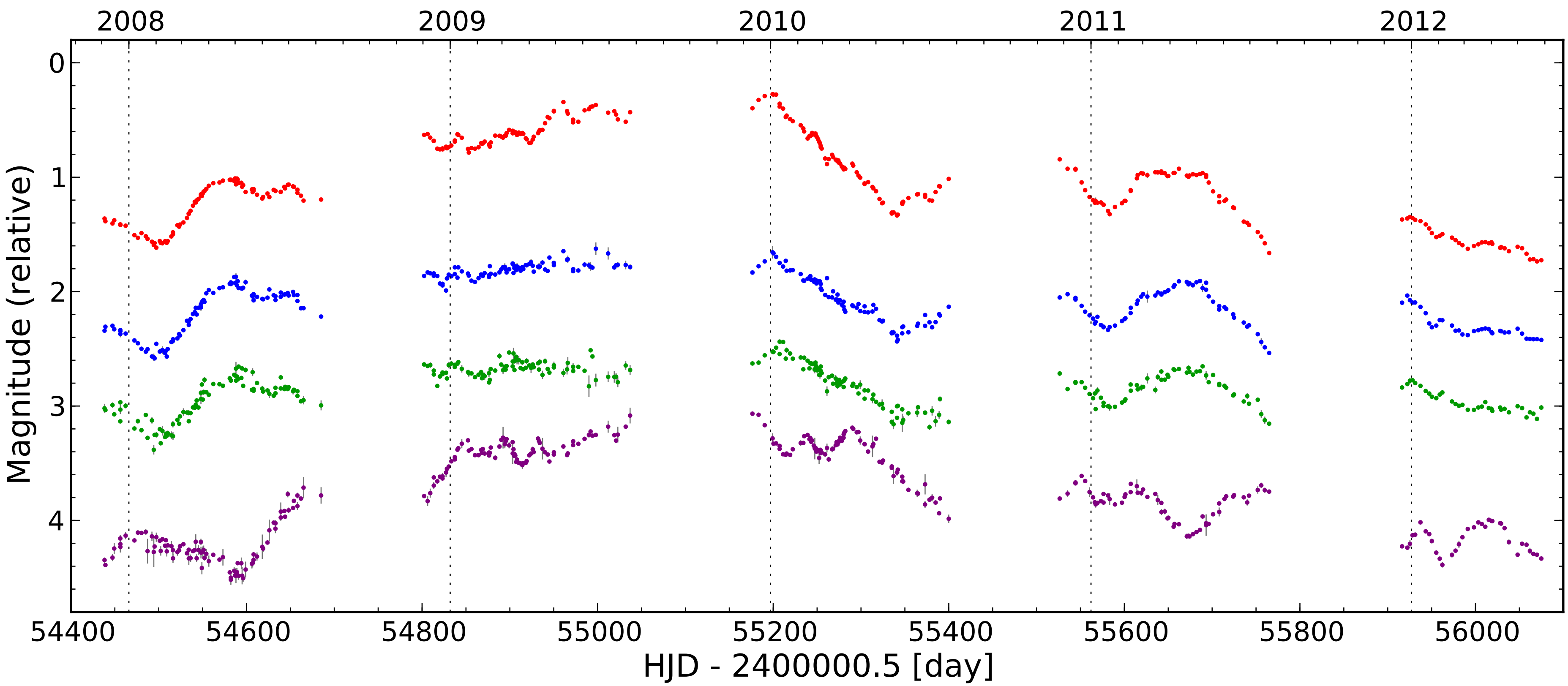

5-10 years lightcurves lead to delays with 2-3% accuracy

LSST should provide measurements for 1000s of systems

Tewes, …, Sluse 2013, A&A, 556, A22

Galaxies lensing galaxies: Sloan Lens ACS survey (SLACS)

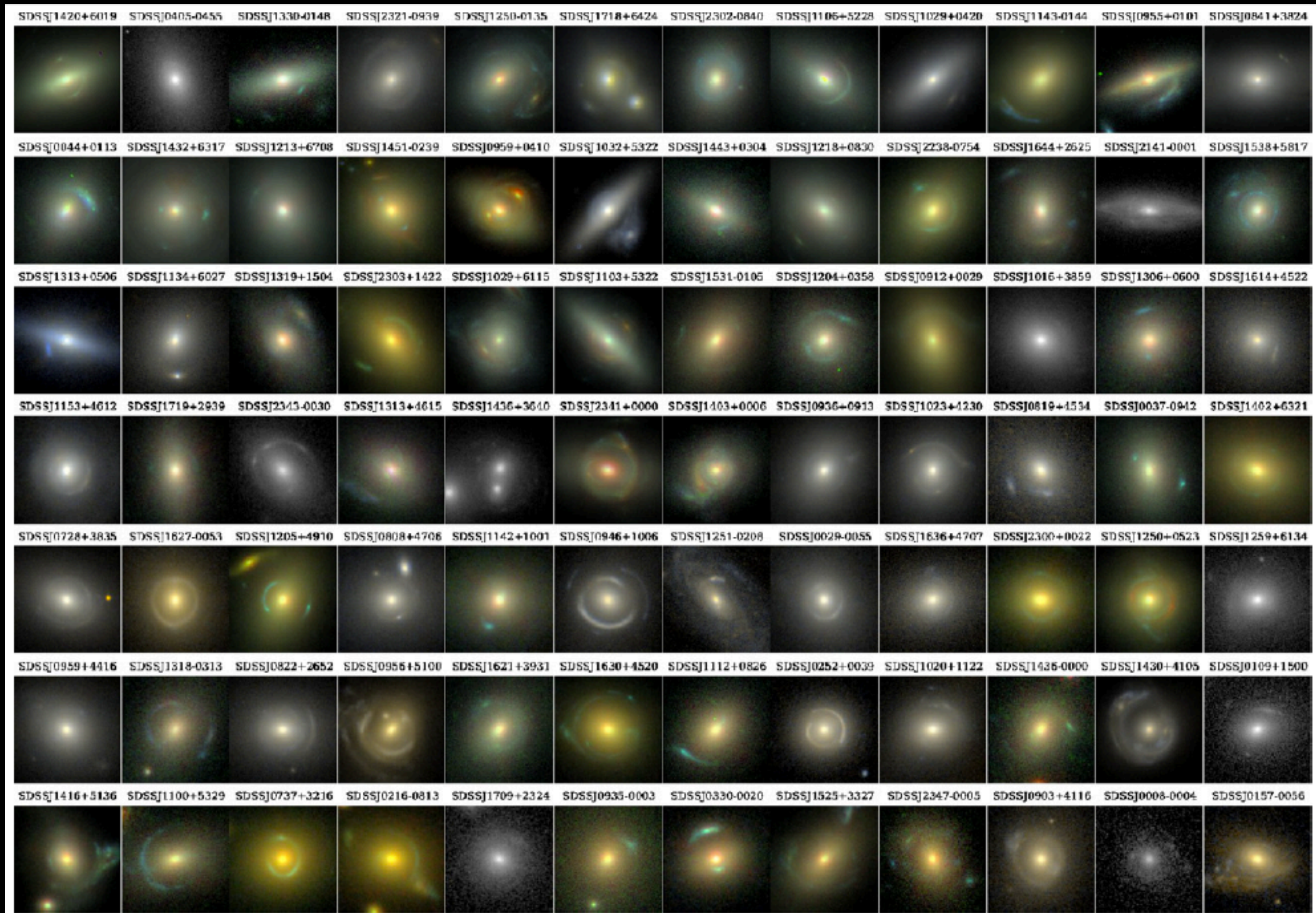

Auger+2009, ApJ, 75, 1099

Combining strong lensing with stellar mass

Stellar mass M_* from Stellar Population Synthesis Model (SPS) + M_{tot} from lensing
=> f_{DM} , $\Upsilon = M/L$

Lens vs Stellar masses in 57 SLACS lenses
(dotted ········ : $M_L = M_*$)

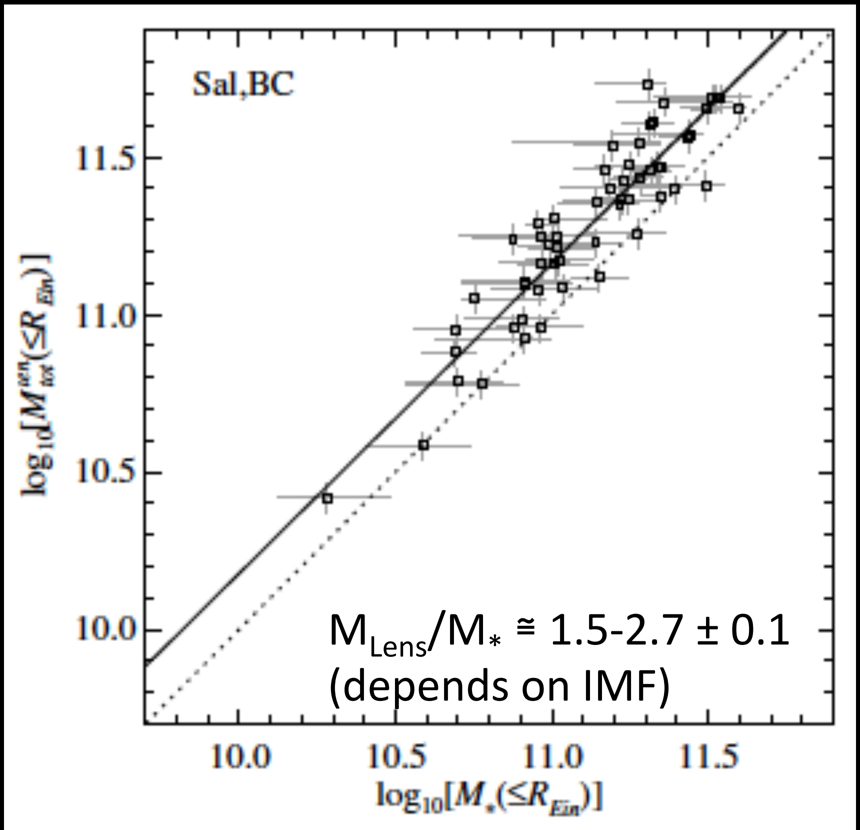

f_{DM} (< r_e) for SLACS lenses
Salpeter (red)– Chabrier (black) IMF

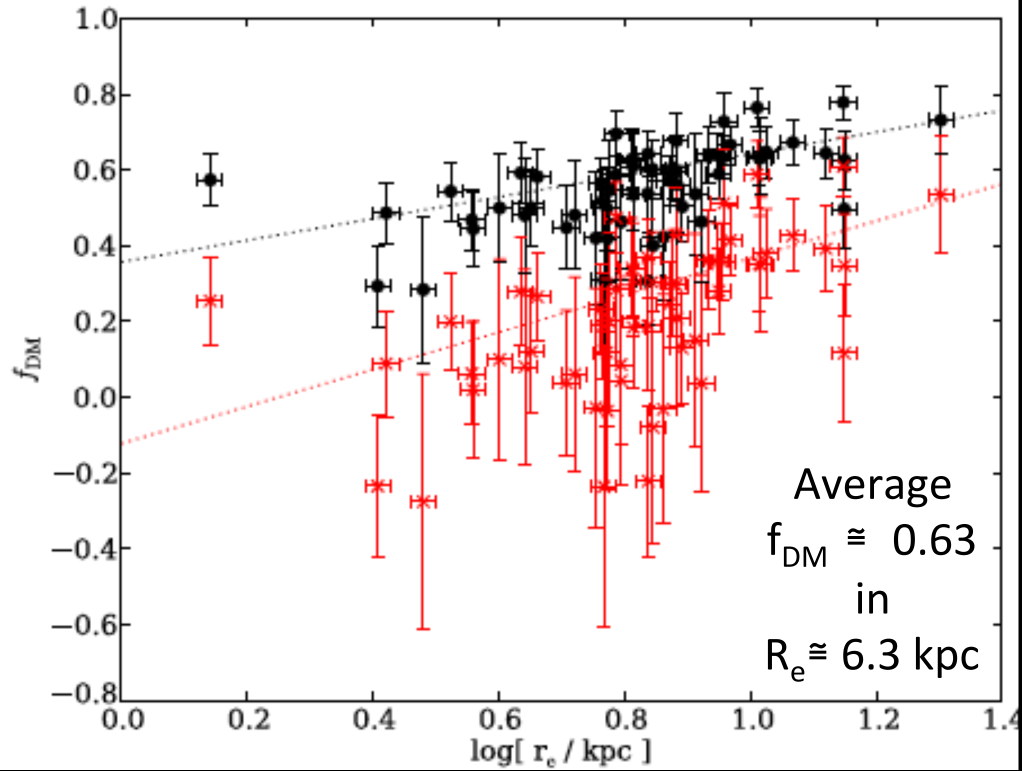

Grillo+ 2009 A&A, 401, 561; Auger+2010, ApJ, 724, 511

Combining strong lensing mass and dynamical mass

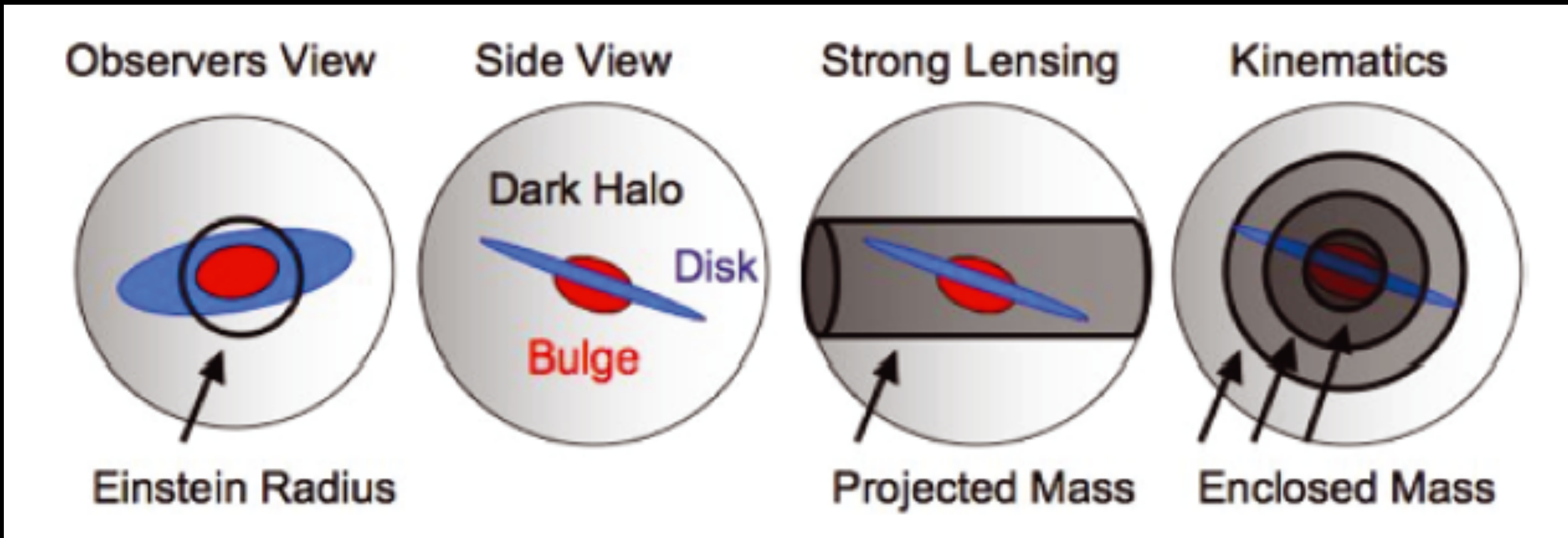

Dynamical mass M_{dyn} within R_{eff} and strong lensing mass $M(<R_E)$
=> slope γ of the density profile

Dutton+2011, MNRAS, 417, 1621

Combining strong lensing mass and dynamical mass

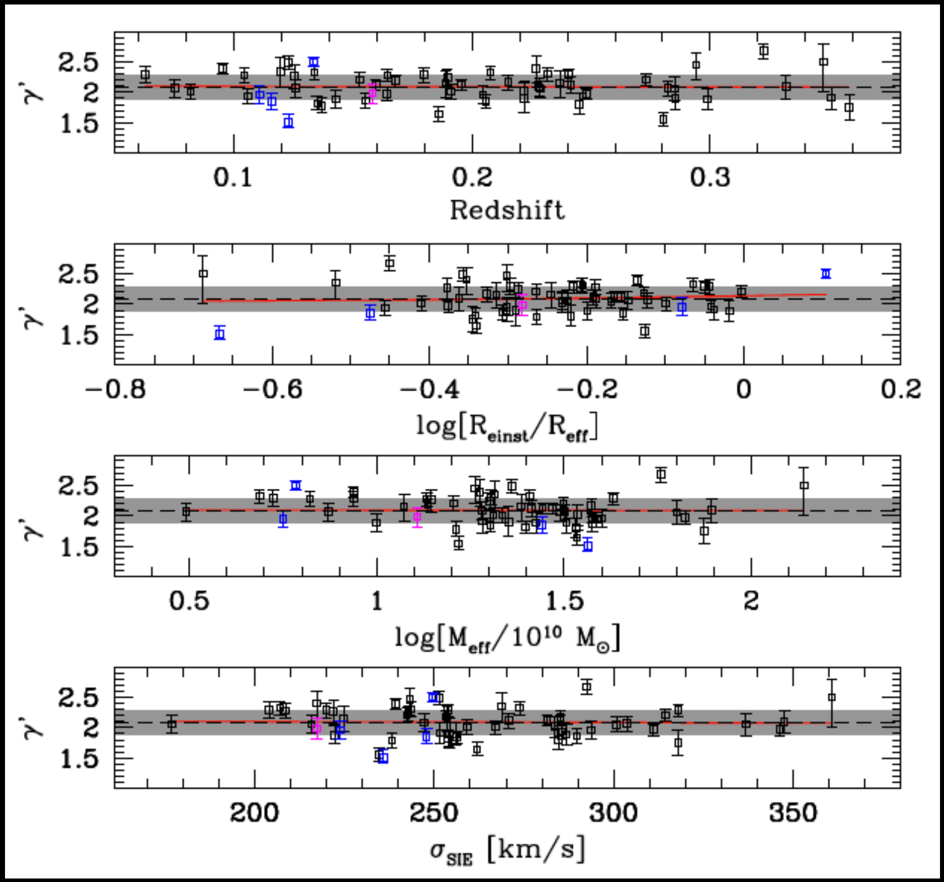

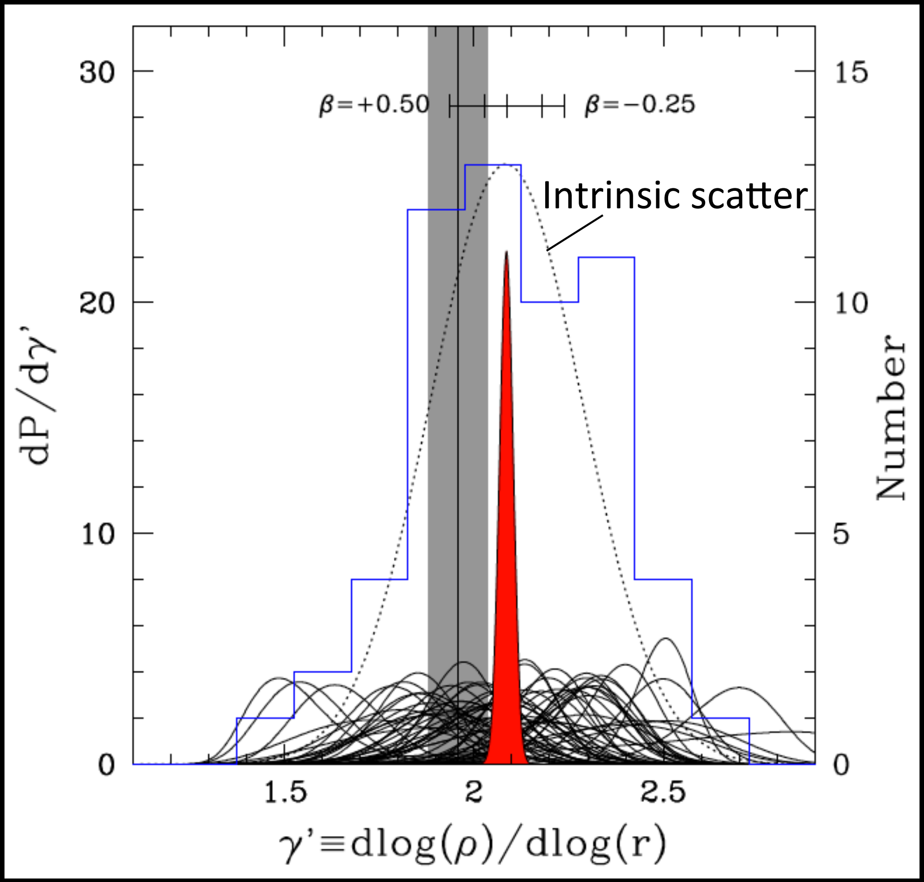

$\gamma = 2.085 \pm 0.025\ \text{(rand)} \pm 0.1\text{(sys)}$

Koopmans+ 2009, ApJL, 703, 51

Combining strong lensing mass and dynamical mass

SLACS – BELLS – SL2S samples

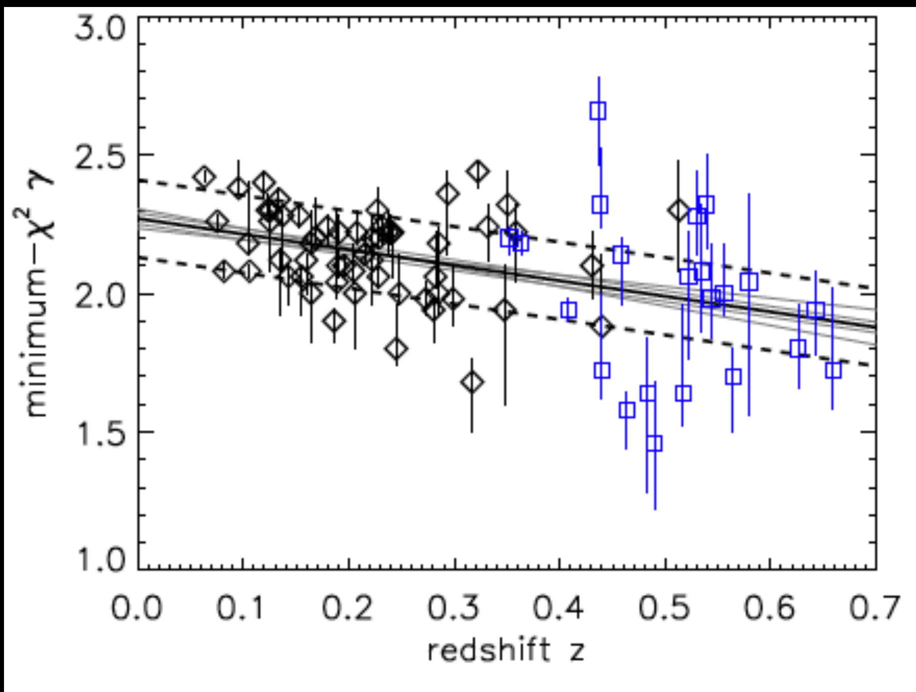

Bolton+ 2012, ApJ, 757, 82

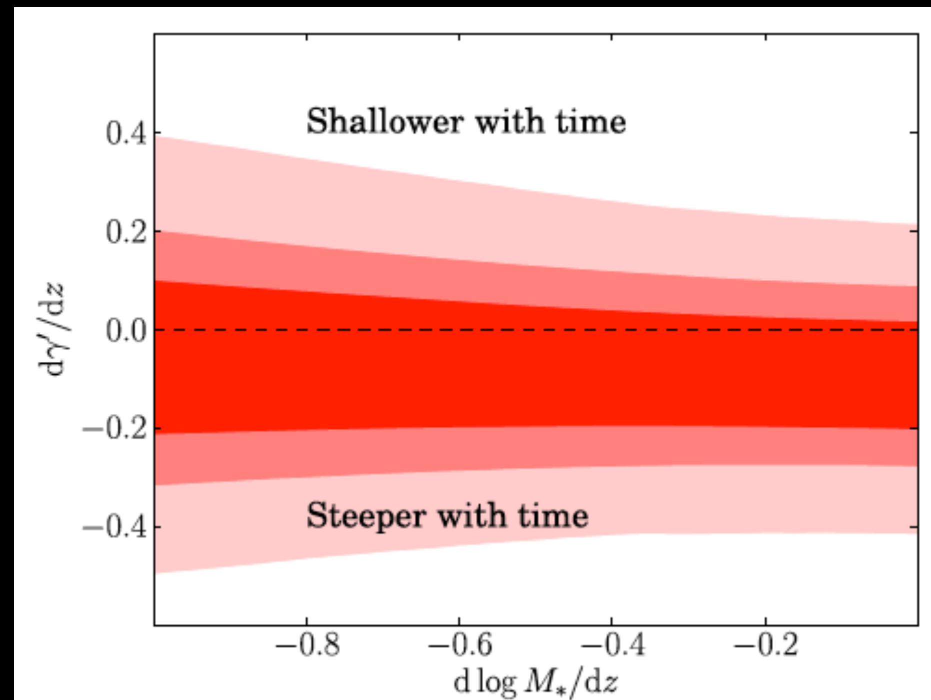

Sonnenfeld+ 2013, ApJ, 777, 98

Apparent evolution of the mean slope γ' with redshift (steeper profiles recently) **BUT** this also reflects a change of stellar density and stellar mass: galaxies grow in M_* but decrease in Σ_* from z = 1 to 0, while preserving γ'.

Slope from single object with time-delay

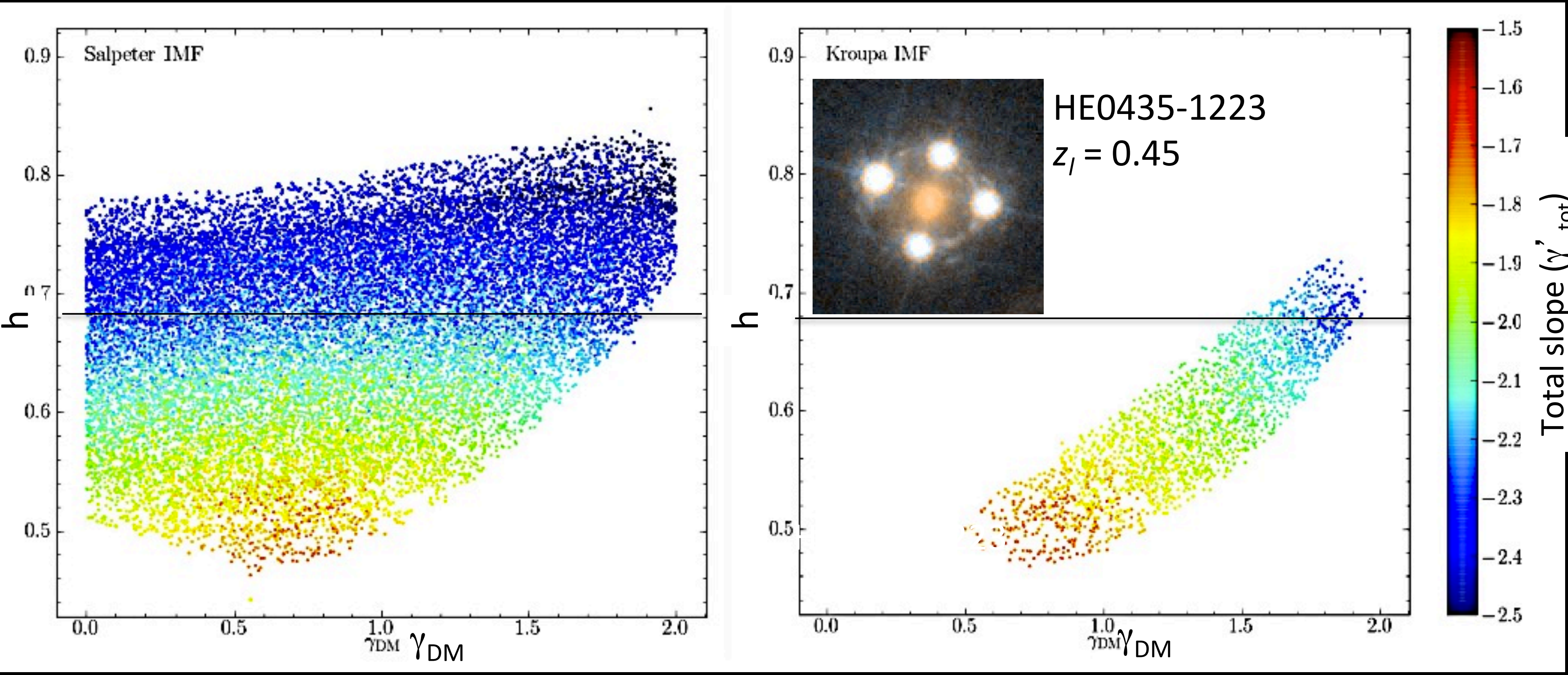

In concordance cosmology, γ' = 2.1± 0.1, while γ_{DM} depends more of the IMF

Courbin, Chantry, Revaz, Sluse+ 2011, A&A, 536, A53

Mass-Sheet Transformation (MST)

$$\kappa_\lambda(\theta) = \lambda\kappa(\theta) + (1-\lambda)$$

Source position: $\beta \rightarrow \lambda\beta$

Delay: $H_0\Delta t \rightarrow \lambda H_0 \Delta t$

Magnification: $\mu \rightarrow \mu / \lambda^2$

$$\psi_\lambda(\theta) = \frac{1-\lambda}{2}|\theta|^2 + \lambda\,\psi(\theta)$$

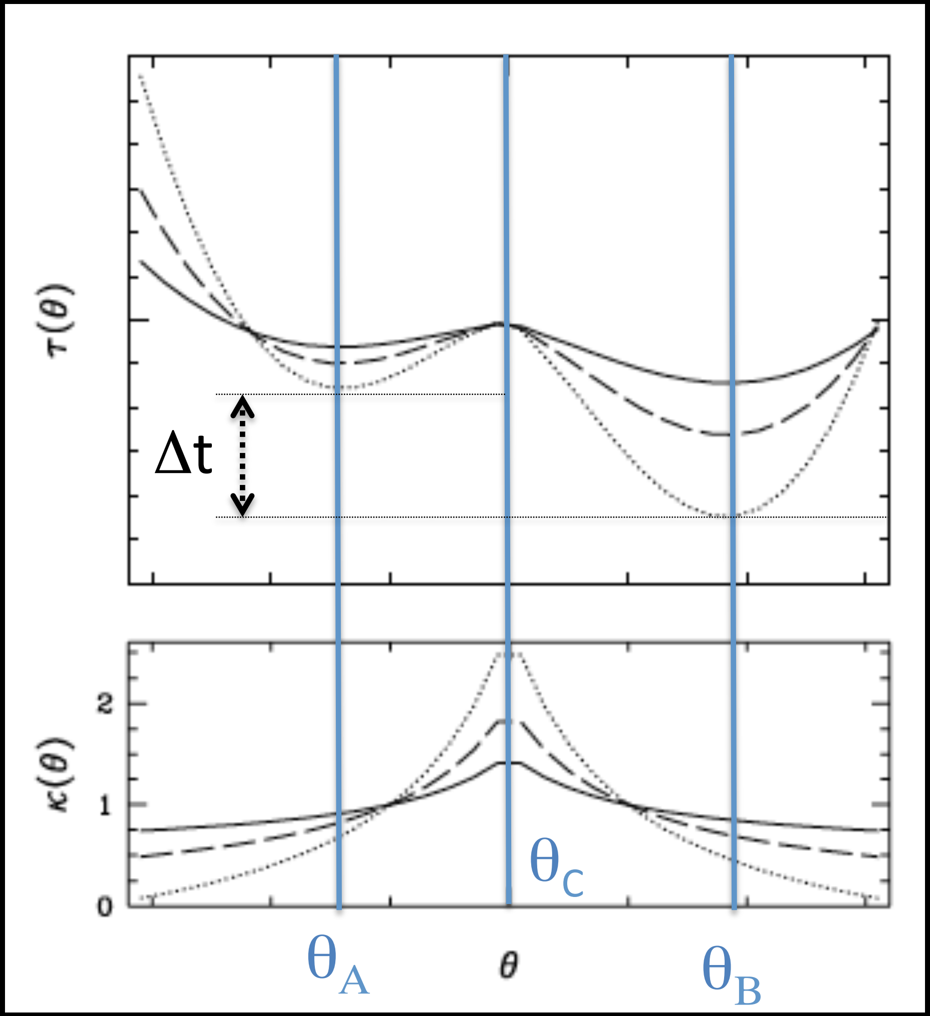

Falco et al. 1985, Gorenstein et al. 1988, …

Courbin+ 2002, LNP, 608

Illustration of the MST at work

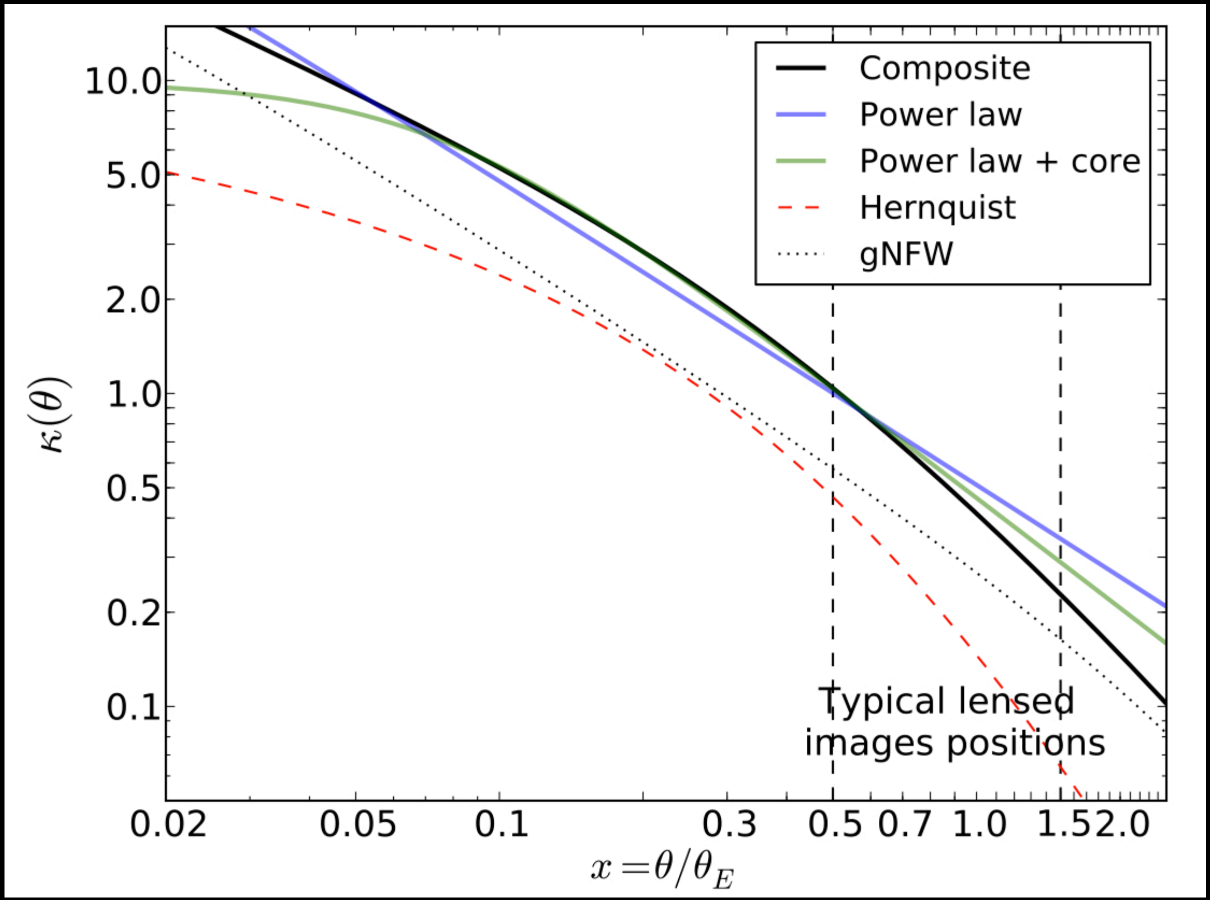

DM + Baryons (=Composite) is close to PL and can be transformed into PL via a MST

Δt breaks the MST !

Schneider & Sluse 2013, A&A, 559, A37
Schneider & Sluse 2014, A&A, 564, A103

Testing density profile with Illustris simulations

- Box size: (106.5 Mpc)^3
- Mass resolution: $6.26\times10^{6} M_{\odot}$
- Gravitational softening length 710 pc; hydrodynamical element size of 48 pc
- Resolve 40 000 galaxies with a variety of morphologies and reproduce LF, TF relations etc.

Illustris Lensing catalogue:
Einstein radius, dark matter fraction, 2D and 3D logarithmic slopes, effective radius, ellipticity, RA, l.o.s. stellar velocity dispersion, anisotropic parameter, dark halo mass, stellar mass etc.

Mock Illustris lensing systems

Xu, Sluse, et al. 2015, in preparation

Testing the PL model with Illustris simulations

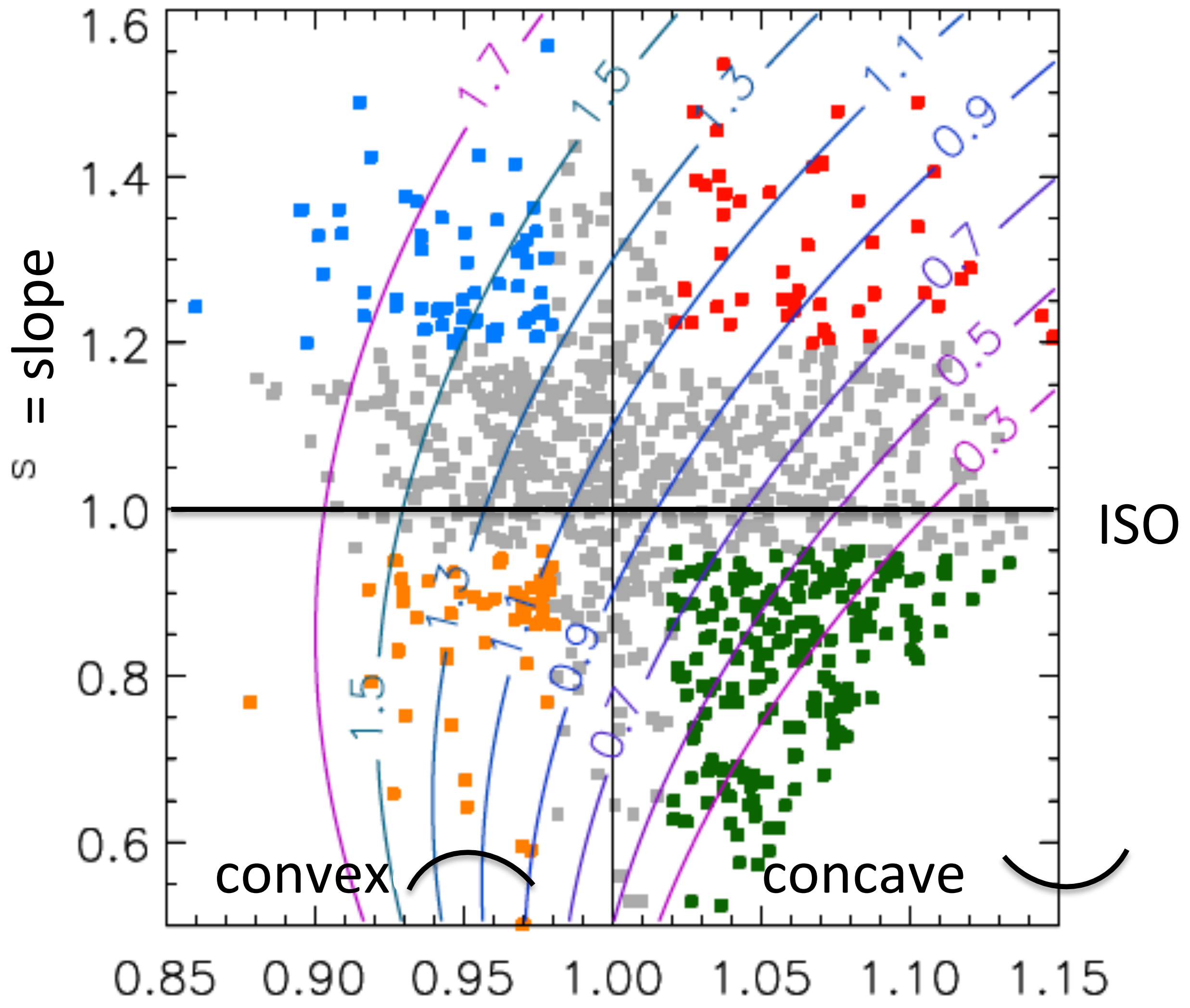

Xu, Sluse, et al. 2015, in preparation

$z_l = 0.2$

$z_s = 1.5$

Flux ratio in lensed quasars

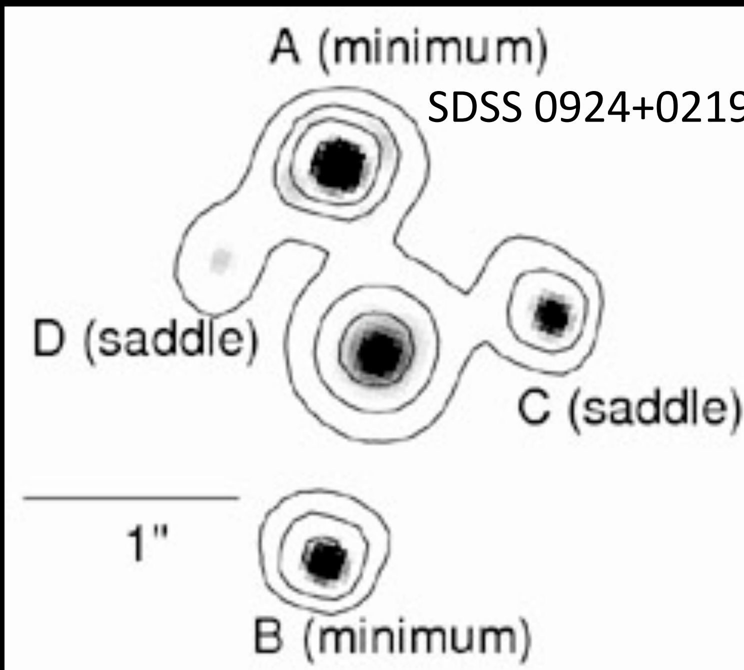

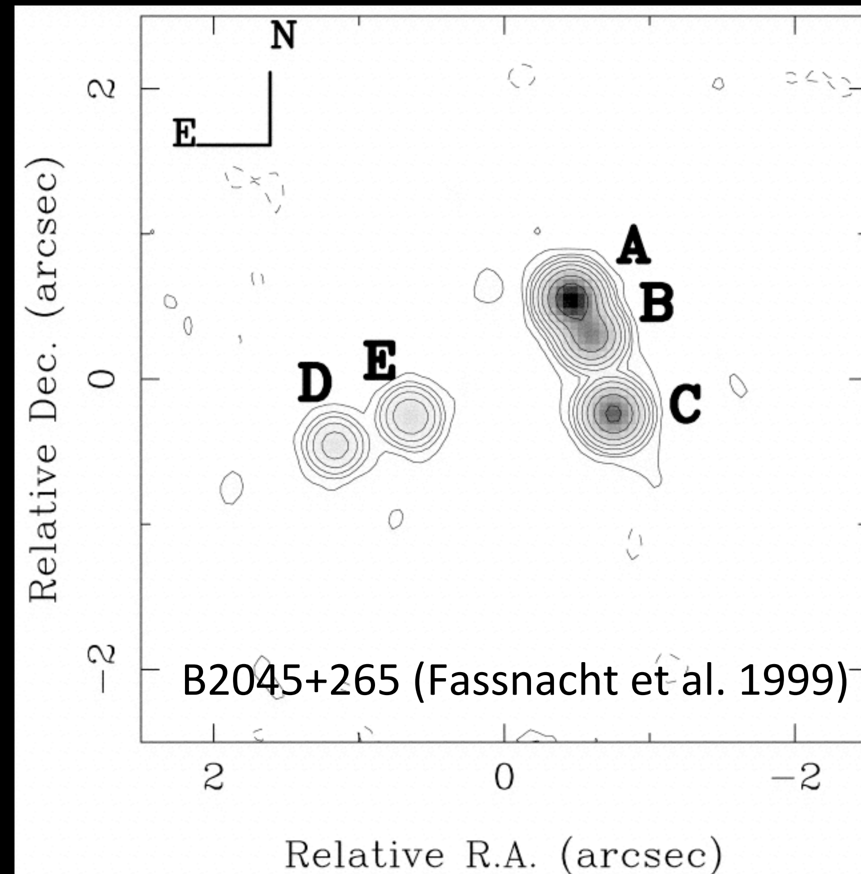

Flux ratio anomalies in lensed quasars

Dark matter substructures

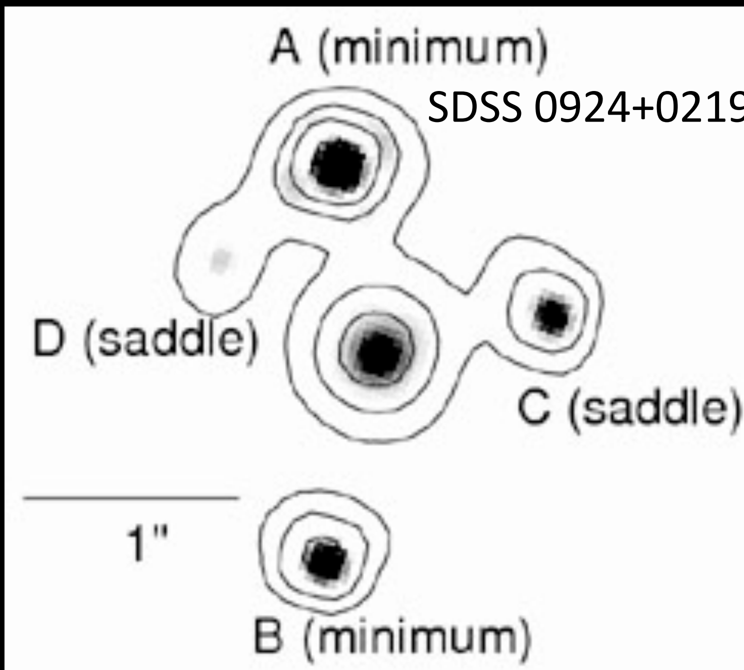

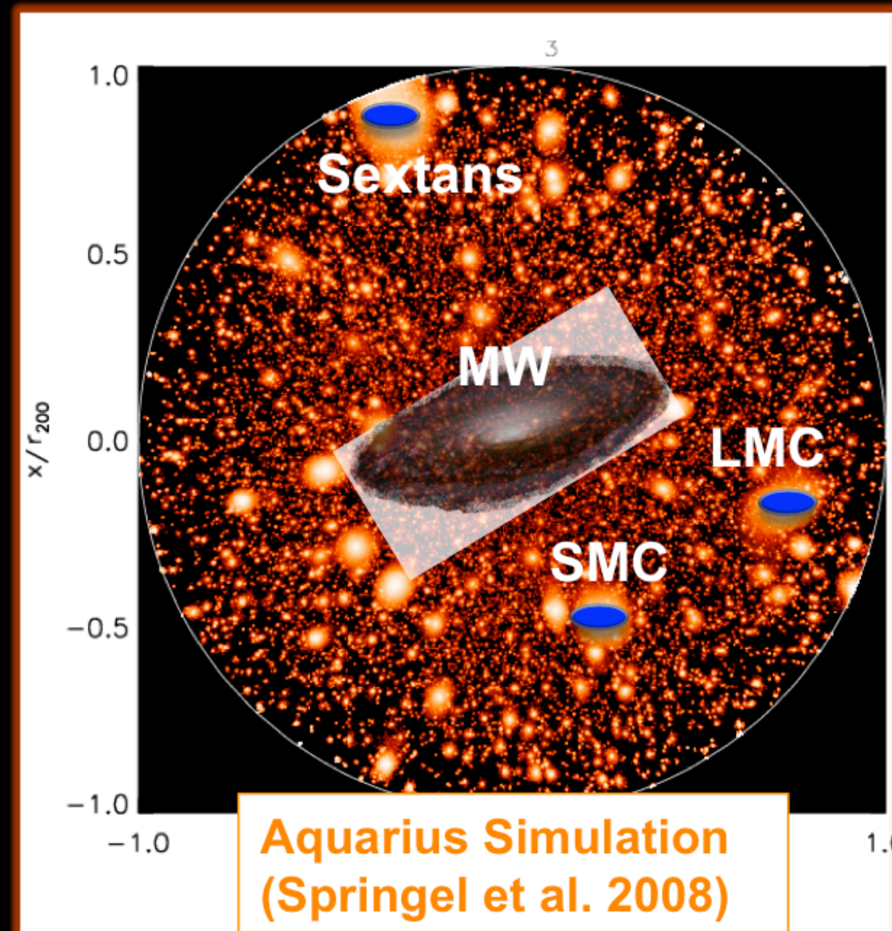

How frequently the flux ratio anomaly happens reflects how abundant the dark matter substructures are in the lens galaxy and its host dark halo

Flux ratio anomalies in lensed quasars

Dark matter substructures

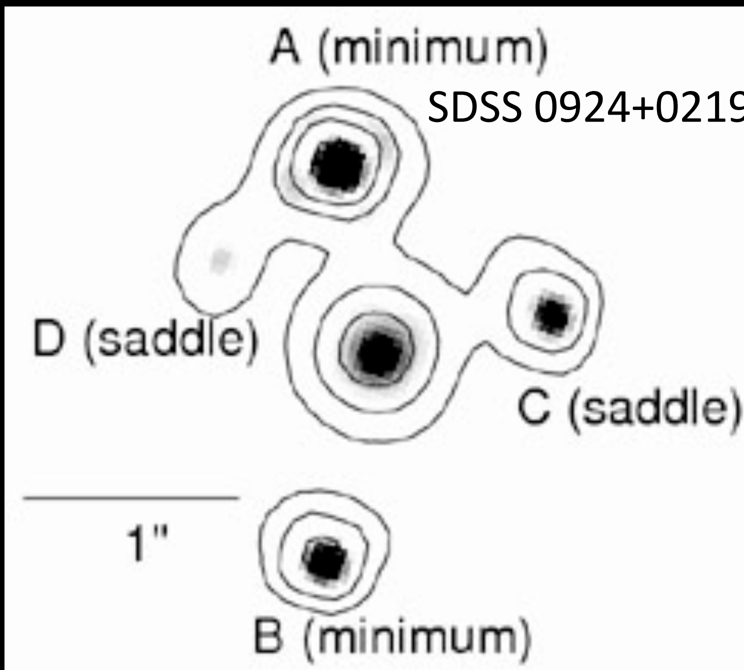

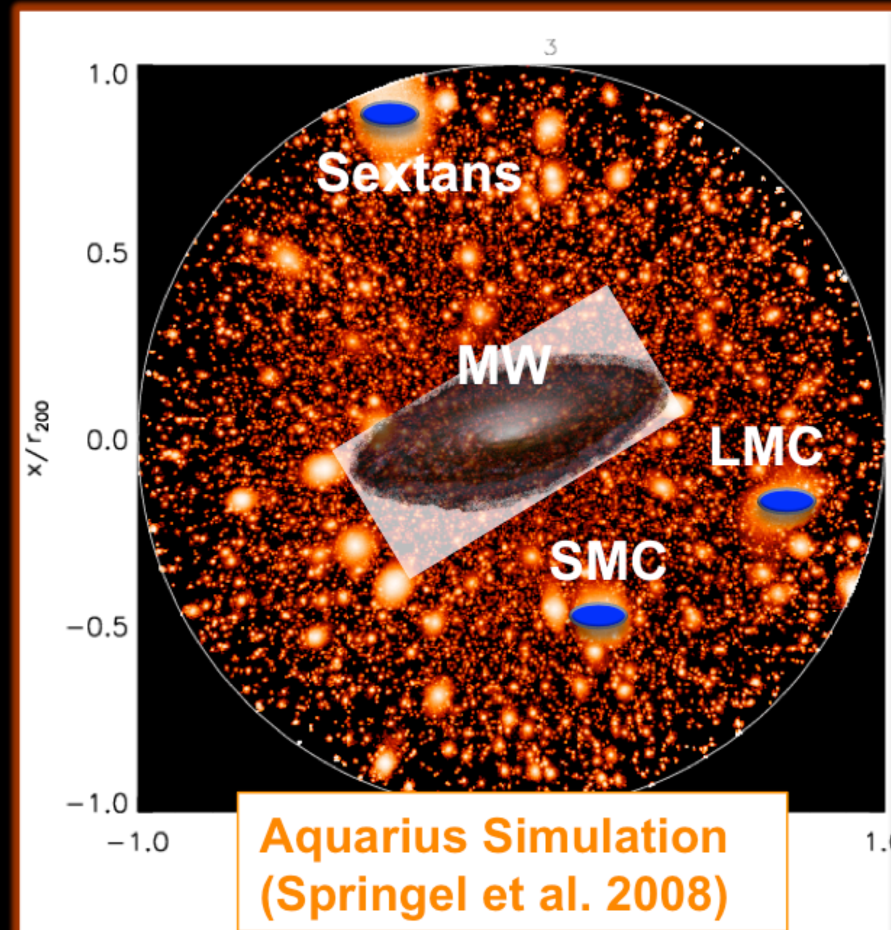

Comparison of radio anomalies with CDM simulations (Aquarius+Phoenix) suggest that the observed frequency is compatible with ΛCDM but possibility of increased rate of anomalies due to disks and/or boxyness of density profiles

Xu, Sluse, et al. 2015, MNRAS, 447, 3189

Back to the source

Principle of the lens inversion

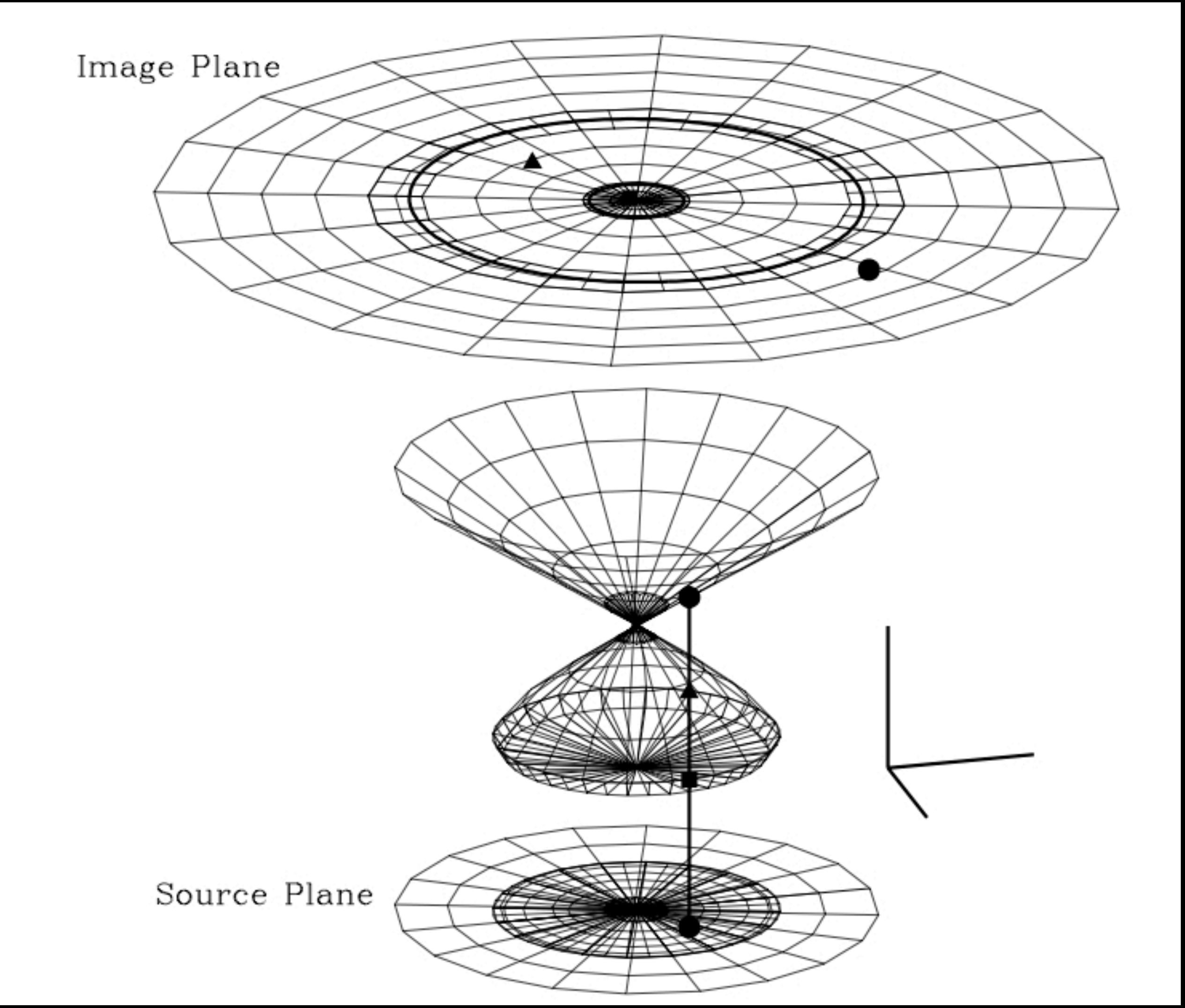

Credits
C. Keeton

Back to the source

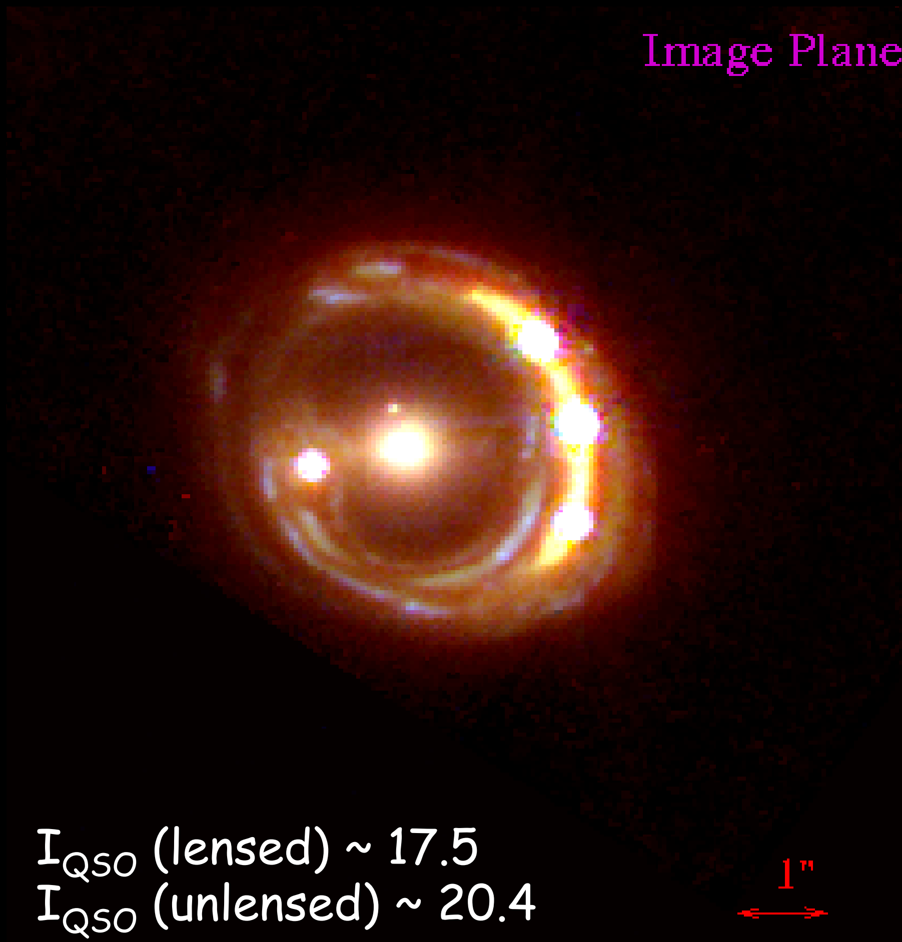

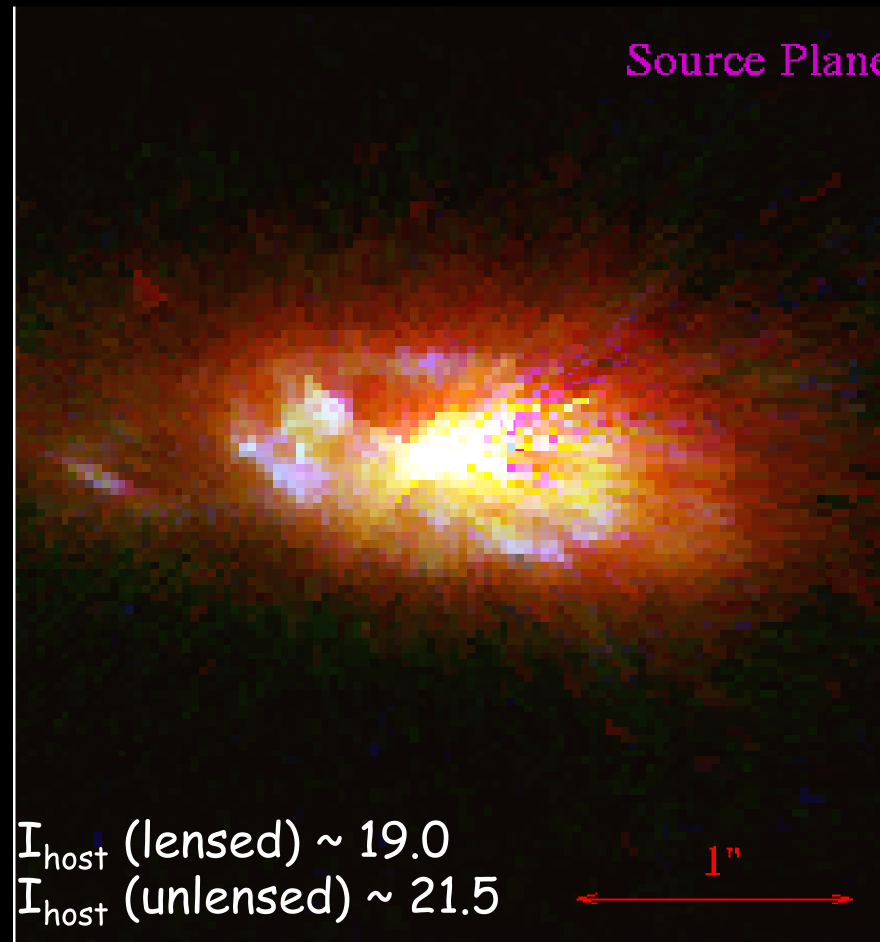

Resolution ~ 0.1'' ~ 0.7 kpc

Sluse et al. 2003, A&A, 406, L43

Claeskens, Sluse et al. 2006 A&A, 451, 865

GEMS sample

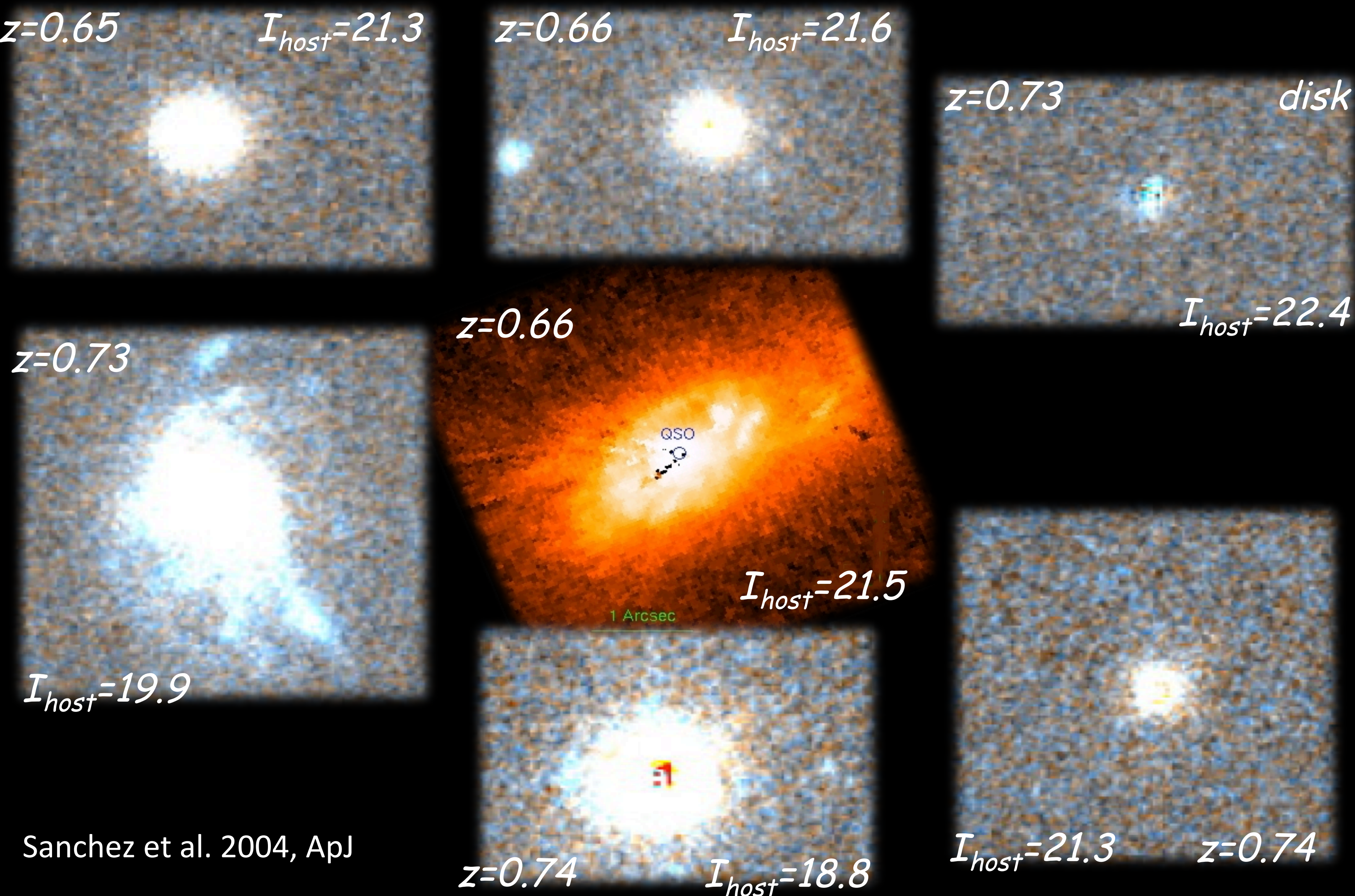

Sanchez et al. 2004, ApJ

Zooming in further into the source ?

MICROLENSING

Micro-lensing: Basics

Macrolensing = multiple images angularly resolved ($\Delta\theta \sim 1$ arcsec) = STRONG lensing

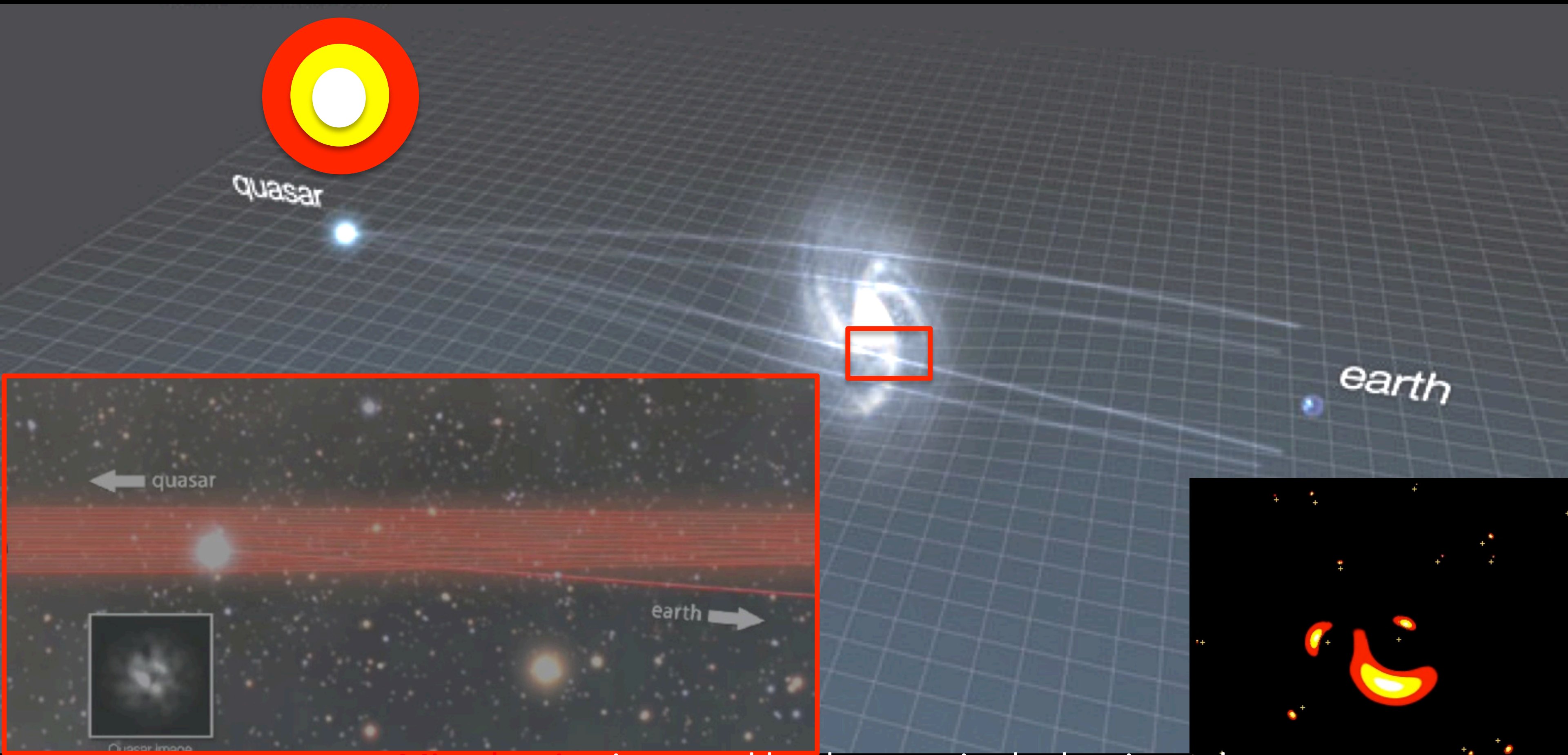

Microlensing is caused by the stars in the lensing galaxy

=

unresolved microlensed images ($\Delta\theta \sim 1$ μas)

AGNs: Overview

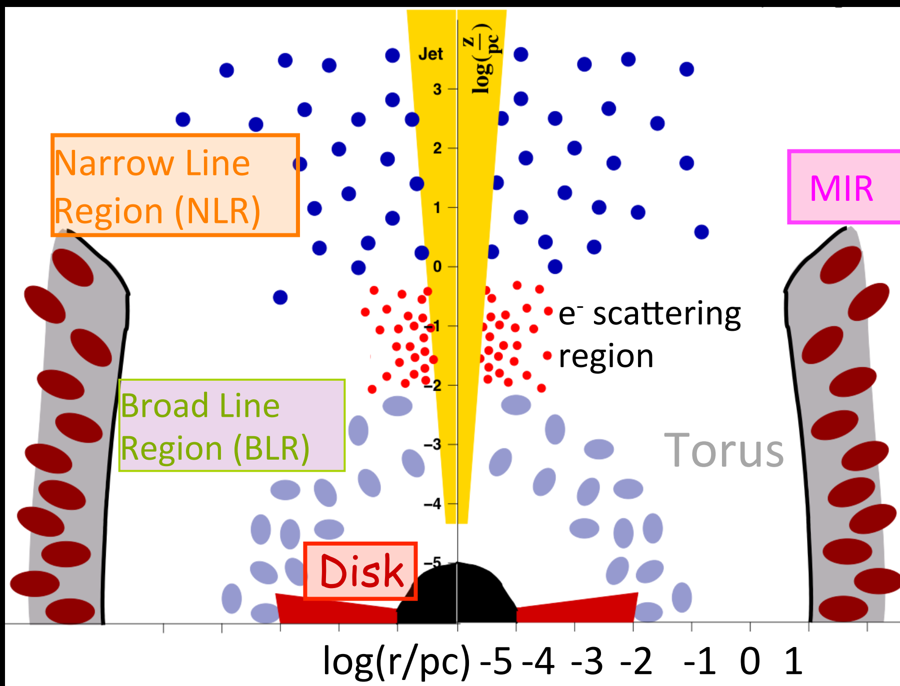

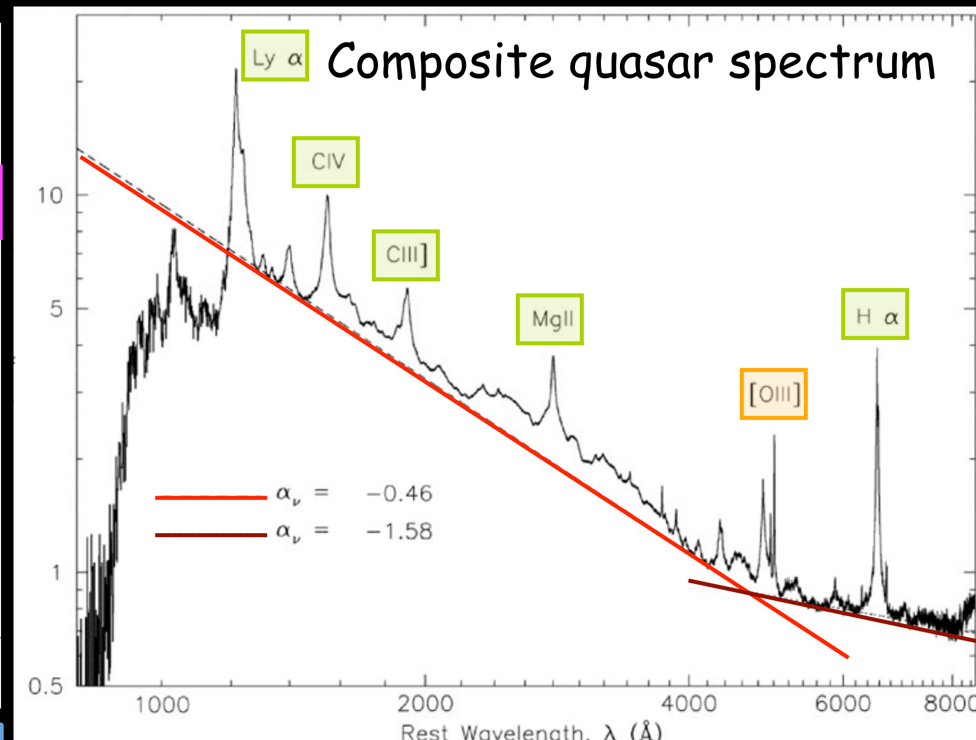

Vanden Berk et al. 2001, AJ, 122, 549

Today: ~ 10 mas ~ 80 pc resolution (z=3; AO)
~ 1-0.1 pc (VLTI, low z)

Future: 0.1 mas ~ 0.8 pc resolution (z =3)

Microlensing: 0.04 pc resolution (up to z=4)

BLR: FWHM > 2000 km/s
NLR: FWHM < 1000 km/s

Microlensing in the Einstein Cross

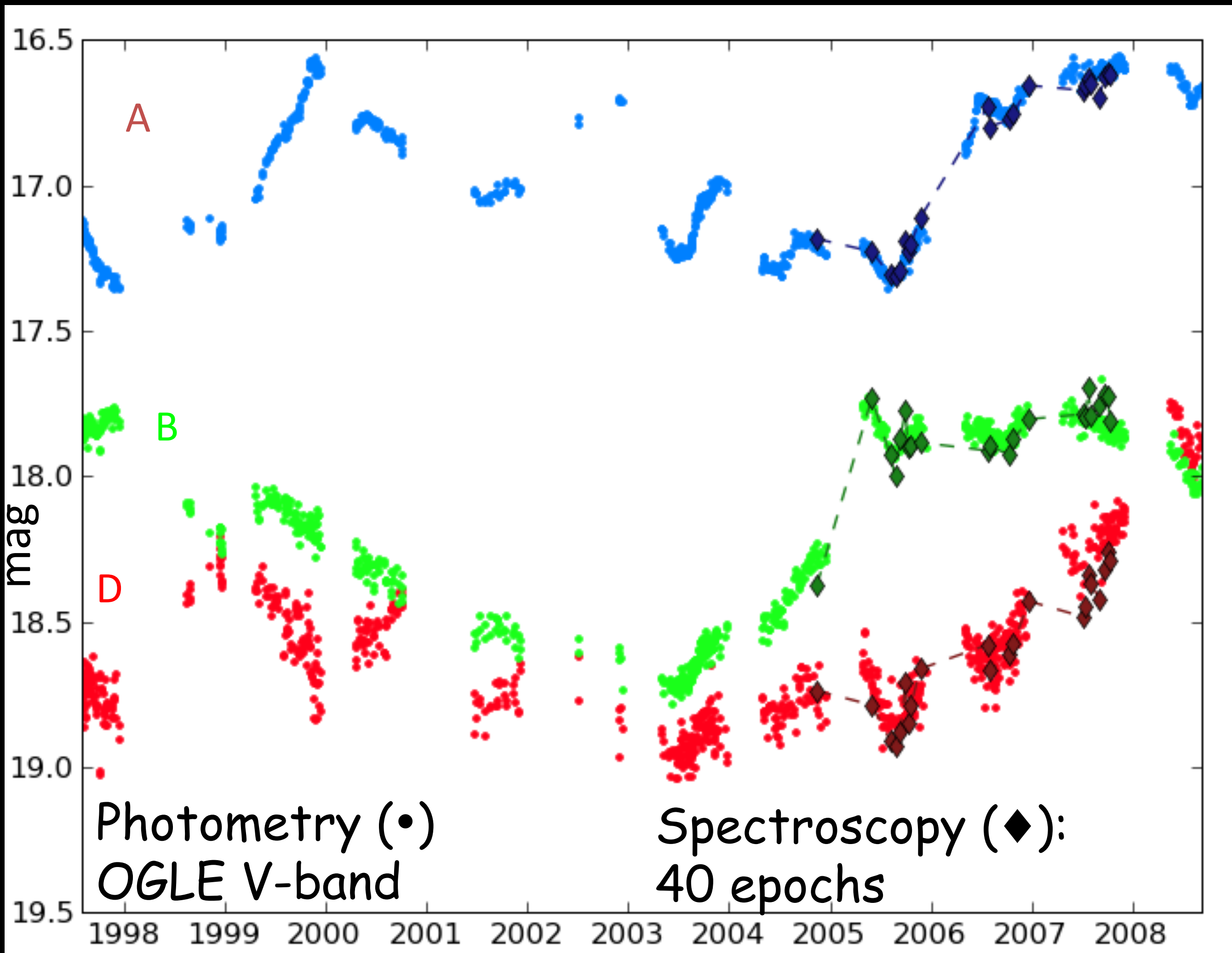

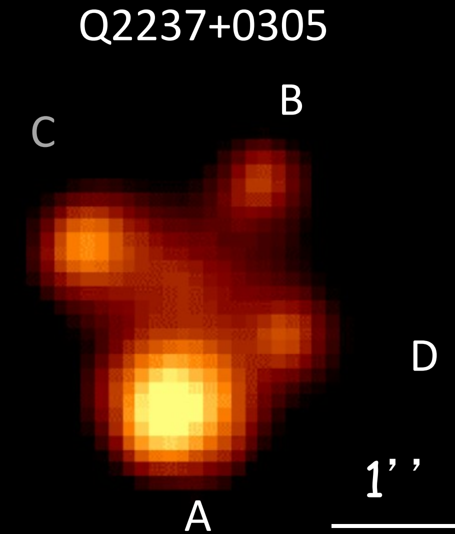

$z_s = 1.695$ $z_l = 0.039$

Time delay $\Delta t < 1$ day

Eigenbrod, Courbin, Sluse+ 2008a, A&A 480, 647

Microlensing in the Einstein Cross

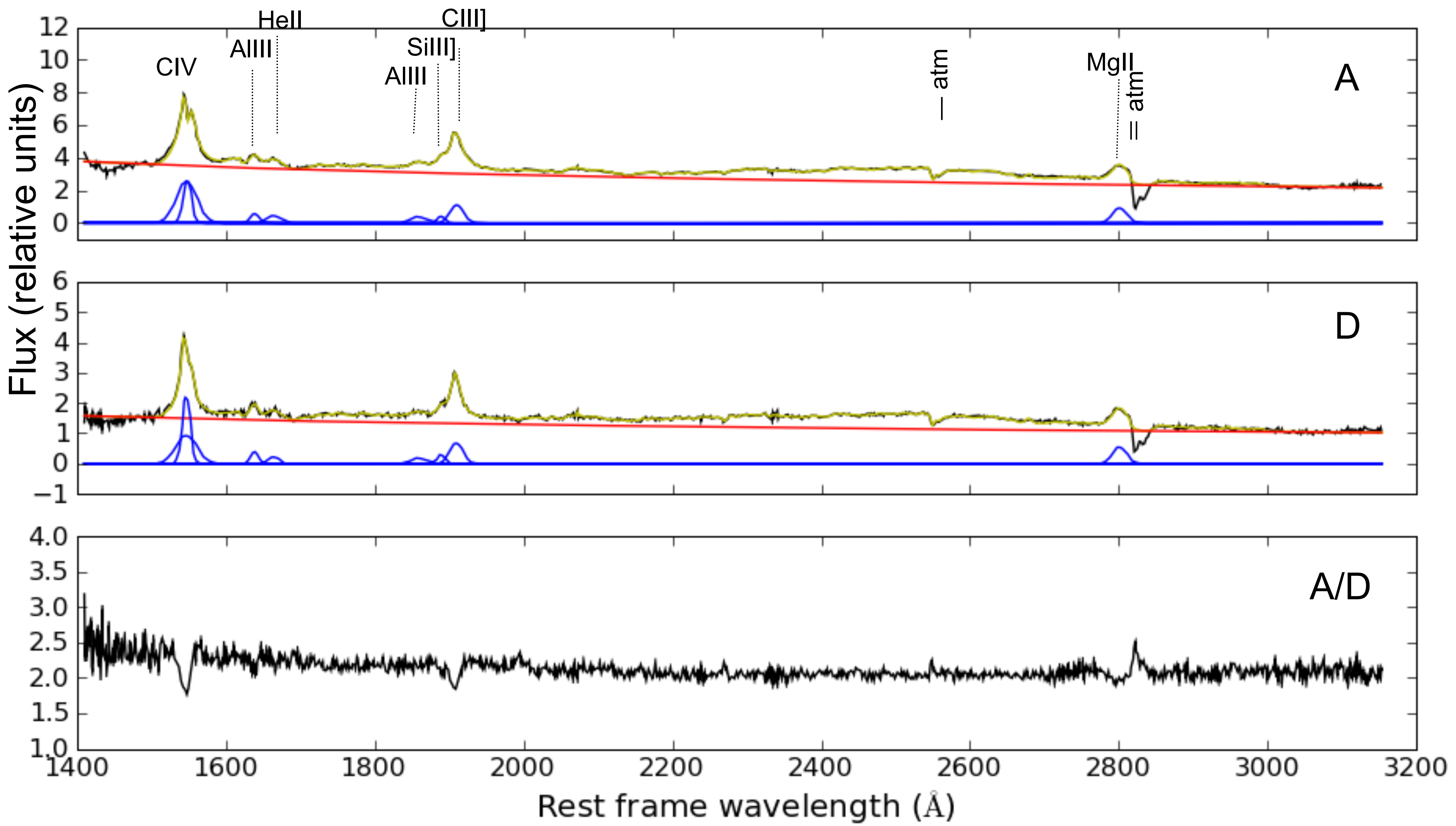

Eigenbrod, Courbin, Sluse+ 2008a, A&A 480, 647

Microlensing in the Einstein Cross: Accretion disc

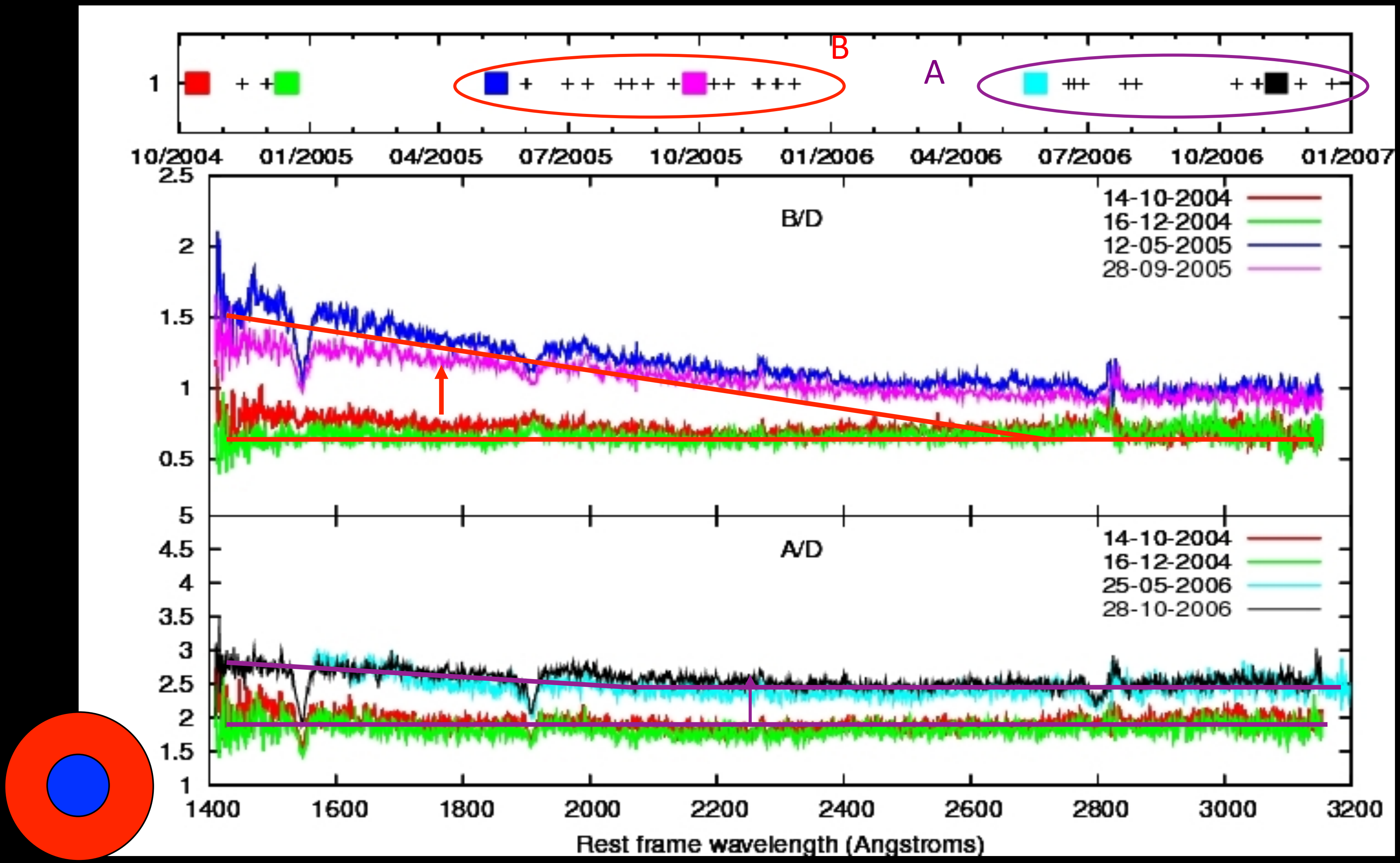

Microlensing in the Einstein Cross: Accretion disc

Observed micro-lensed induced chromatic variations of the continuum

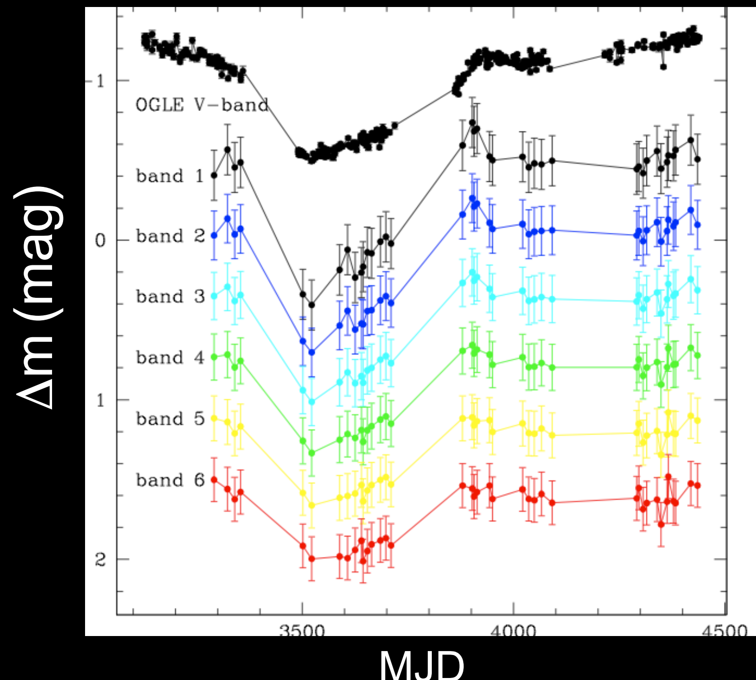

ML simulations

Results of the simulation

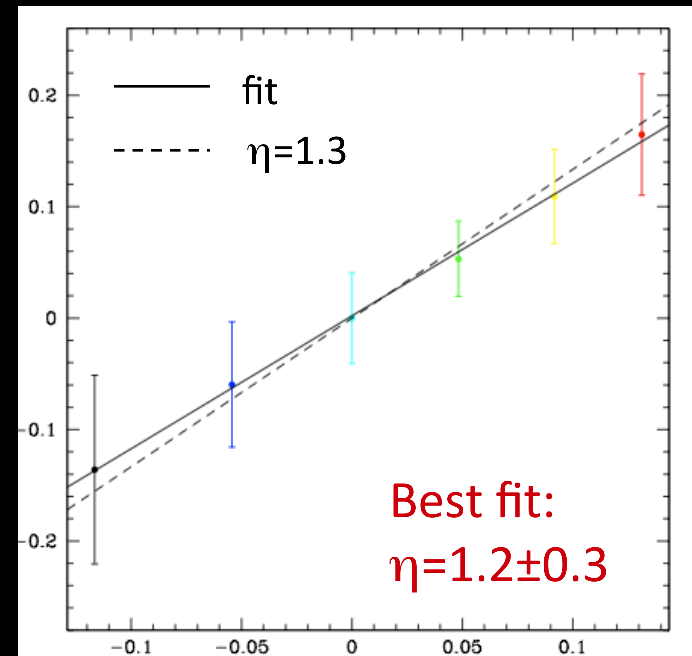

Accretion disk model:

$$\frac{R}{R_{\mathrm{ref}}} = \left(\frac{\lambda}{\lambda_{\mathrm{ref}}} \right)^{\eta}$$

η= 1.3 (Shakura & Sunayev, 1973)
η= 1.15 (Agol & Krolik, 2000)
η= 1.75 (Gaskell 2008)

Eigenbrod+ 2008, A&A 490, 933

Microlensing in other systems: Accretion disc

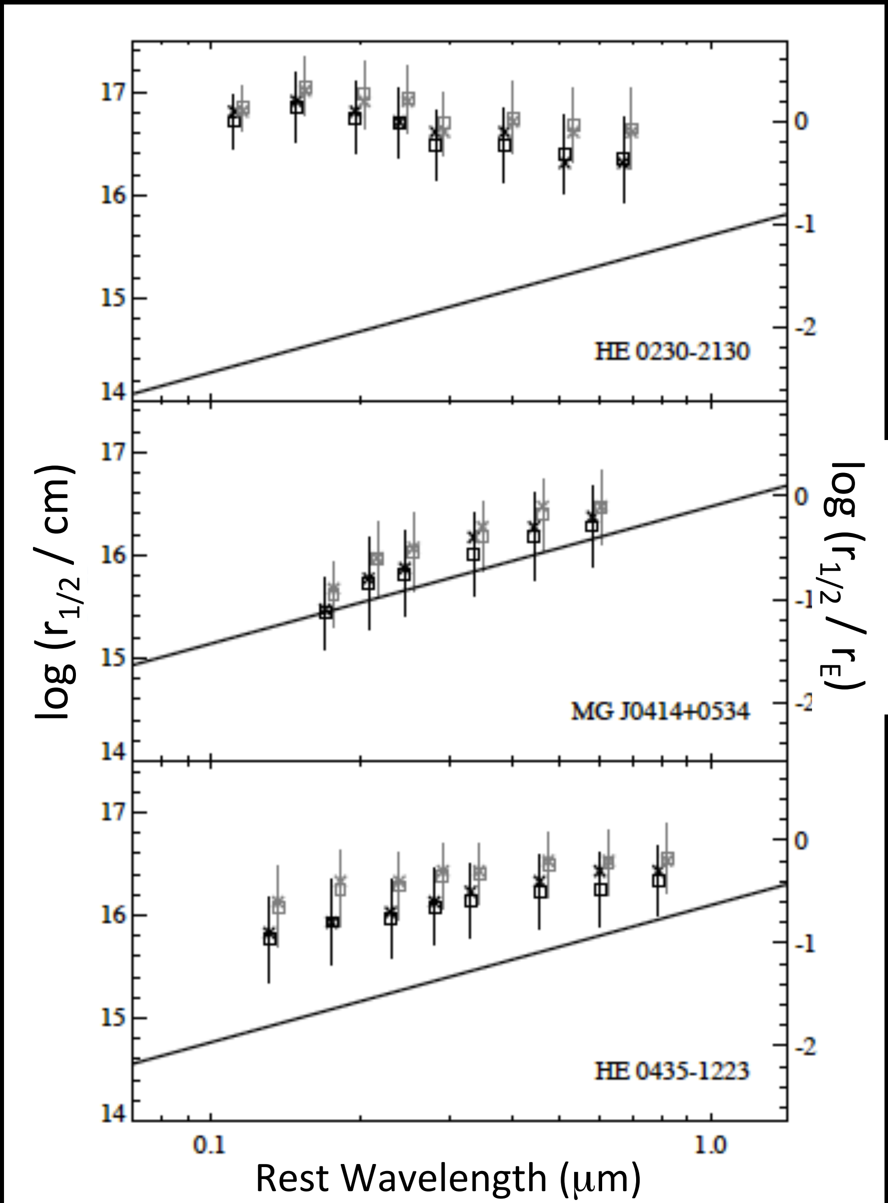

ML sizes generally larger than expected from theory, and slopes steeper than Shakura Sunyaev (e.g. Morgan et al. 2010, Blackburne et al. 2011)

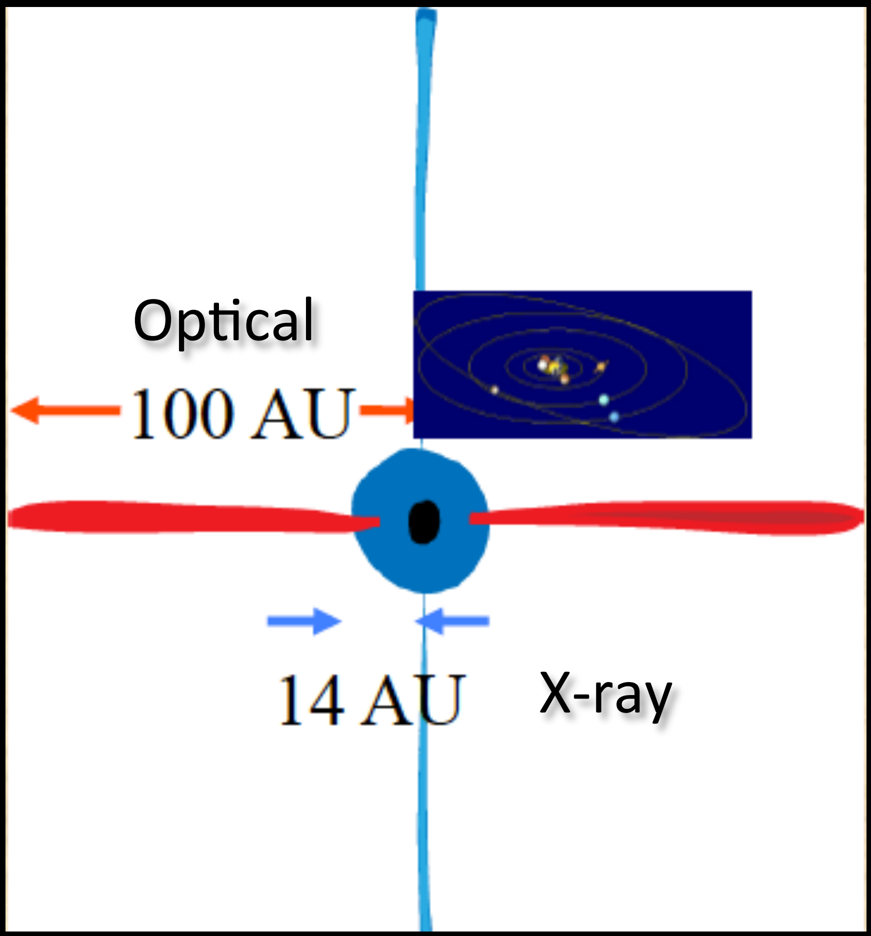

Microlensing also depends on the local f_{DM}

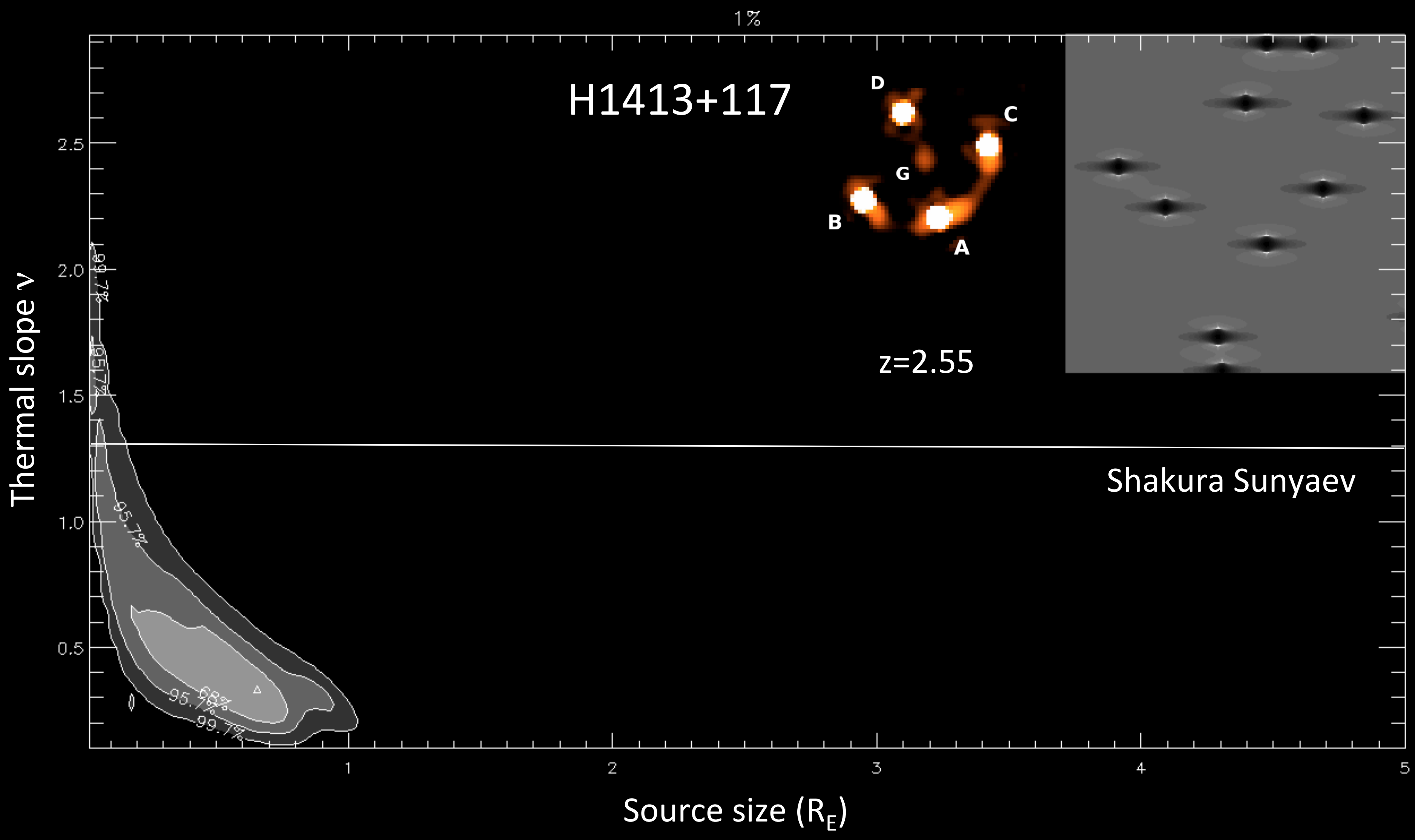

Sluse+ 2015, (in prep)

Microlensing in the Einstein Cross: The BLR

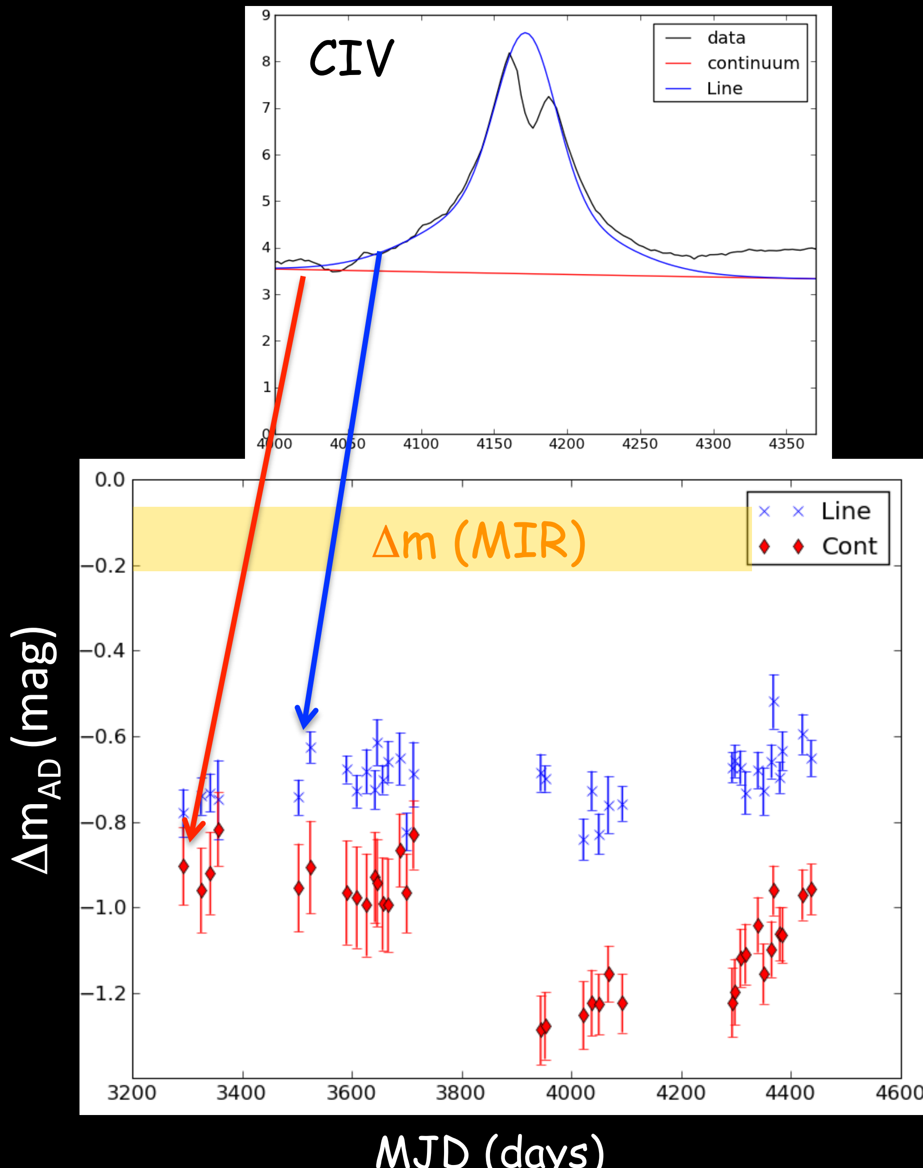

Size of the BLR: Comparison of the observed lightcurve with mL simu.: $R_{CIV} \sim 66\ (\langle M \rangle / 0.3 M_{\odot})^{1/2}$ lt-days

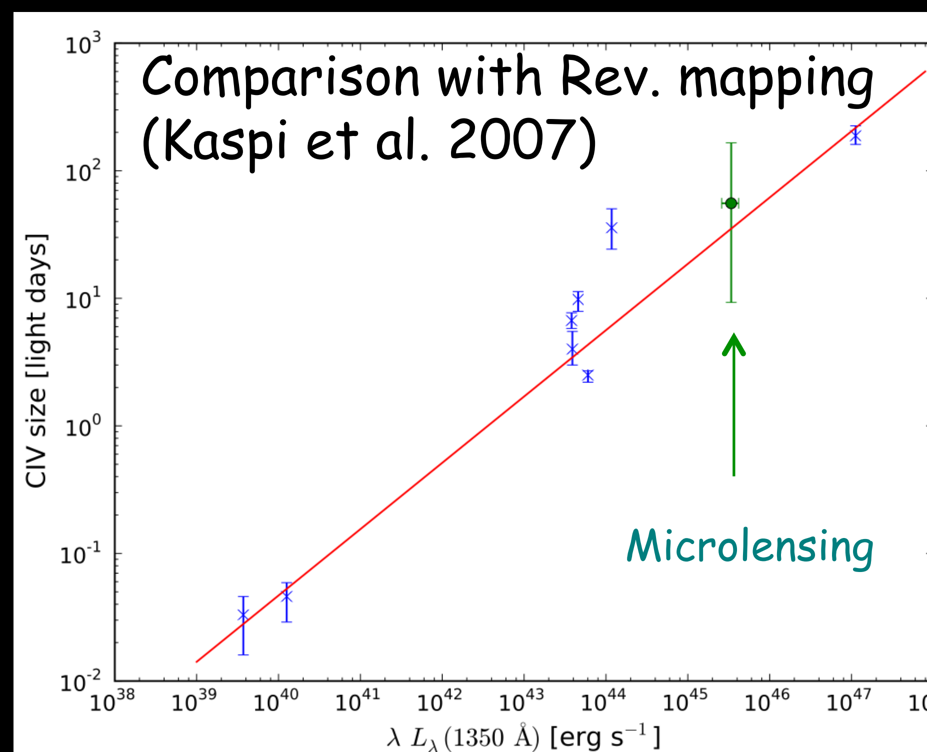

Sluse+ 2011, A&A 528 A100

Microlensing of the BLR

CIV Spectral decomposition

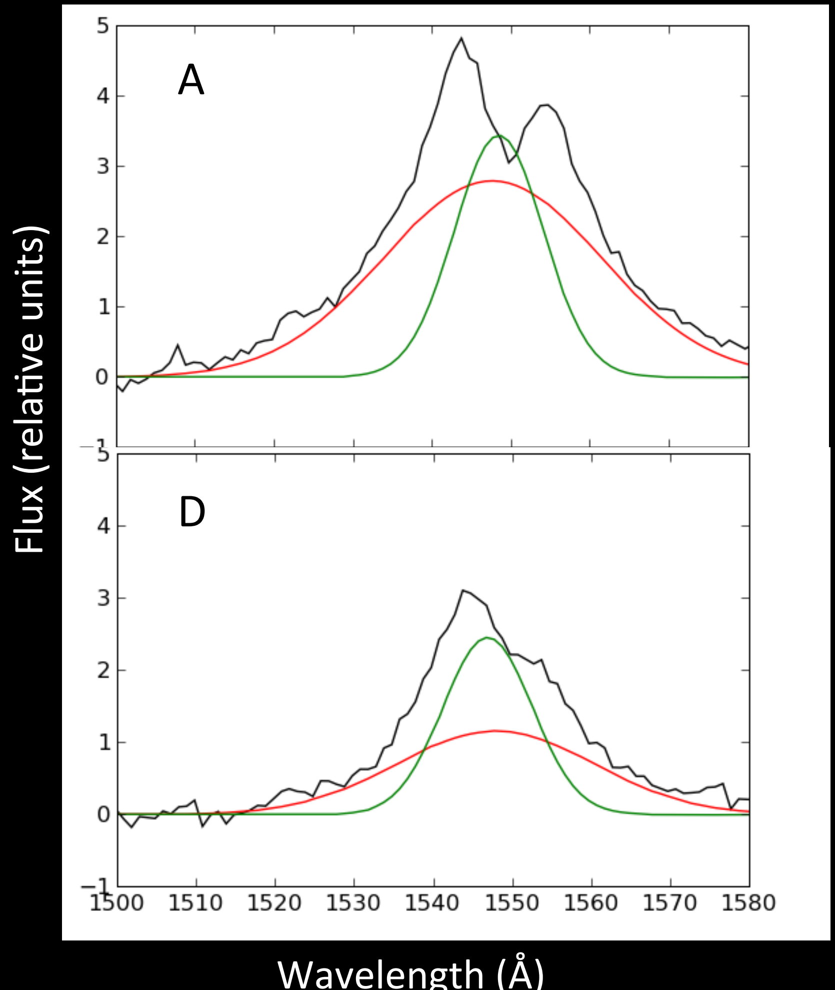

The broadest component of the line (higher velocity) is also the most microlensed, hence the most compact (only about 4 times larger than the AD)

In many systems, only the red/blue wing of the line is microlensed => BLR is not spherically symmetric (geometry+velocity field).

Sluse+ 2011, A&A 528 A100
Sluse+ 2012, A&A 544, A62

Conclusions

1. One of the most accurate measurement of the mass of galaxies up to z=1 (typically 5% accuracy within 1 $R_E \cong$ 5-10 kpc)

2. Projected DM fraction within inner 5 kpc of elliptical galaxies, and slope of the total (baryon+DM) density profile:

   $f_{DM} \cong$ 0.63 within $R_e \cong$ 6.3 kpc (for Salpeter IMF)

   $\gamma = 2.085 \pm 0.025$ (rand) $\pm$ 0.1(sys) (up to $z \cong$ 0.3)

3. Structure of distant sources (quasars, galaxies) from kpc scales down to sub-pc scales (AD+BLR+host in the same systems !) :
   AD: ML size generally larger than theory size; slope steeper than SS
   BLR: compatible with local reverberation mapping measurements (but up to high z) + sensitivity to the geometry of the BLR.